





Article

The Volcanic Geoheritage in the Pristine Natural Environment of Harrat Lunayyir, Saudi Arabia: Opportunities for Geotourism and Geohazard Issues

Károly Németh ^{1,2,3,*} , Abdulrahman Sowaigh ¹, Vladyslav Zakharovskiy ³ , Mostafa Toni ⁴ , Mahmoud Ashor ¹, Vladimir Sokolov ¹, Fawaz Moqem ¹, Khalid Abdulhafaz ¹, Turki Hablil ¹, Turki Sehli ¹ and Khalid Yousef ¹ 

¹ Saudi Geological Survey, Geohazard Research Unit, Jeddah 21514, Saudi Arabia; sowaigh.ag@sgs.gov.sa (A.S.); ashor.ms@sgs.gov.sa (M.A.); sokolov.v@sgs.gov.sa (V.S.); moqem.fa@sgs.gov.sa (F.M.); abdulhafez.kh@sgs.gov.sa (K.A.); hablil.ty@sgs.gov.sa (T.H.); sehli.ta@sgs.gov.sa (T.S.); yousef.kh@sgs.gov.sa (K.Y.)

² Institute of Earth Physics and Space Science, 9400 Sopron, Hungary

³ Volcanic Risk Solutions, Massey University, Palmerston North 4442, New Zealand; v.zakharovskiy@massey.ac.nz

⁴ Geology Department, Faculty of Sciences, Helwan University, Cairo 11281, Egypt; mostafa.toni@science.helwan.edu.eg

* Correspondence: k.nemeth@massey.ac.nz; Tel.: +966-567634717

Abstract

The Lunayyir Volcanic Field (Harrat Lunayyir), located on the western boundary of the Arabian Microplate, comprises a Quaternary volcanic region featuring approximately 150 volcanoes formed from around 700 vents. In 2009, a significant volcano-seismic event occurred, resulting in the formation of a nearly 20 km long fissure. Geophysical modeling has demonstrated that this area lies above an eruptible magma system, unequivocally confirming ongoing volcanic activity. Recent geological mapping and age determinations have further established the field as a young Quaternary volcanic landscape. Notably, the 2009 event provided critical evidence of the region's volcanic activity and underscored the potential to connect its volcanic geoheritage with hazard mitigation strategies. The volcanic field displays diverse features, including effusive eruptions—primarily pāhoehoe and ‘a‘a lava flows—and explosive structures such as spatter ramparts and multi-crater scoria cones. While effusive eruptions are most common and exert long-term impacts, explosive eruptions tend to be less intense; however, some events have reached a Volcanic Explosivity Index (VEI) of 4, distributing ash up to 250 km. Recognizing the geoheritage and geodiversity of the area may enhance resilience to volcanic hazards through geoconservation, educational initiatives, managed visitation, and establishment of a geoheritage reserve to preserve site conditions. Hazards associated with this dispersed monogenetic volcanic field manifest with recurrence intervals ranging from centuries to millennia, presenting challenges for effective communication. Although eruptions are infrequent, they have the potential to impact regional infrastructure. Documentation of volcanic geoheritage supports hazard communication efforts. Within the northern development sector, 26 geosites have been identified, 22 of which pertain to the Quaternary basaltic volcanic field, each representing a specific hazard and contributing vital information for resilience planning.

Keywords: geodiversity; volcanic hazard; hazard resilience; volcanic field; monogenetic volcano; lava flow



Academic Editor: Mario Bentivenga

Received: 28 July 2025

Revised: 29 August 2025

Accepted: 3 September 2025

Published: 4 September 2025

Citation: Németh, K.; Sowaigh, A.; Zakharovskiy, V.; Toni, M.; Ashor, M.; Sokolov, V.; Moqem, F.; Abdulhafaz, K.; Hablil, T.; Sehli, T.; et al. The Volcanic Geoheritage in the Pristine Natural Environment of Harrat Lunayyir, Saudi Arabia: Opportunities for Geotourism and Geohazard Issues. *Heritage* **2025**, *8*, 363. <https://doi.org/10.3390/heritage8090363>

Copyright: © 2025 by the authors.

Licensee MDPI, Basel, Switzerland.

This article is an open access article distributed under the terms and conditions of the Creative Commons Attribution (CC BY) license

(<https://creativecommons.org/licenses/by/4.0/>).

1. Introduction

In recent decades, research on geological heritage has increased public interest in geological processes through events and publications. Studies have focused on identifying and understanding geosites—locations with notable geological features—which is essential for geoconservation efforts. These studies raise awareness among communities and decision-makers, support legislative development, and contribute to creating databases that aid in preserving and managing geological heritage [1–8]. Interest in geoheritage—its study, protection, and promotion—has grown significantly in academic research and policy. Traditionally, conservation efforts have focused on biotic elements, such as plants and animals, often overlooking abiotic features, including rocks and landforms, which are wrongly assumed to be abundant and unthreatened [9]. Only since the late 1990s has research started addressing these abiotic aspects [10]. The misconception that geological resources are limitless, combined with a focus on immediate concerns over long-term processes, can lead to neglect and irreversible loss of unique landscapes due to poor management [9]. Understanding the space–time evolution of natural systems remains challenging in a society oriented toward the present. Geotourism focused on geological features has grown rapidly in the past twenty years, significantly benefiting rural economies [11–15]. This trend is supported by national and international geopark networks that promote geological heritage and sustainable development [16–18].

Nature-based tourism involves activities that depend on relatively undeveloped (pristine) natural resources like scenery, waterways, wildlife, and cultural heritage [19]. The appeal of a tourist destination is influenced by its relief, climate, water features, flora, fauna, and landscapes [20]. A tourist site can be influenced by both its natural condition and its connections to the region's cultural heritage, with these factors together forming a complex geoheritage environment [21]. Recreational tourism, such as spa culture, often thrives in areas where water interacts with rock, making these regions popular destinations in diverse tourism settings [20]. Tourist attractivity for spa and climatic locations can be assessed using factors such as terrain, hydrology, ecosystems, potential for winter sports, and tourism function, allowing for evaluation based on natural characteristics [22]. These methods are potential candidates for geotourism research, particularly in exploring the connection between natural hazard heritage and tourism potential discussed in this report.

Geoheritage research, protection, and education are receiving increased attention from academic and policy sectors. Geoconservation refers to the conservation, study, protection, and dissemination of knowledge about geoheritage and geodiversity through scientific, technical, administrative, educational, and political actions [9]. Such efforts are adapted based on subject matter, location, objectives, and audience. Activities related to geoheritage and geoconservation may link the preservation of geological objects for current and future use, account for their potential changes over time, and utilize them to demonstrate concepts such as geological time and landscape evolution [9]. Geoconservation planning starts with identifying the focus, which includes geosites and areas of geological interest [9]. “Areas of geological interest” are defined as sites or regions that, while not necessarily unique or rare in terms of geological significance, are relevant for educational, tourism, cultural (for instance the original concept of geosite recognition recommended by Wimbledon, 1995 [10]), or regional planning purposes, and may offer opportunities for local development. These areas, like geosites, can also be targeted for geoconservation measures.

Volcanoes represent significant natural phenomena and attract considerable interest from visitors globally. Volcanic geoheritage illustrates the processes of volcanism through geotourism initiatives [23–31]. Numerous volcanic landscapes are incorporated within protected areas under major UNESCO programs—such as World Heritage Sites, the Global Geoparks Network, and the Man and the Biosphere (MAB) program—highlighting their

geological, biological, and cultural importance. These designations also reflect their roles in sustainable development and engagement with local communities [32–34]. Additionally, the International Union of Geological Sciences (IUGS) has classified the first and second *100 Geological Heritage Sites* to recognize locations of significant international scientific value [35].

Since 2013, Saudi Arabia has shown increased interest in documenting its volcanic geoheritage, particularly the extensive Quaternary monogenetic volcanic fields in the western regions—one of the largest such provinces globally [36,37]. Two monogenetic volcanoes from this area were recently included in the first and second *100 IUGS Geological Heritage Sites* [https://iugs-geoheritage.org/geoheritage_sites/historic-scoria-cone-of-the-jabal-qidr/ and https://iugs-geoheritage.org/geoheritage_sites/the-pleistocene-al-wahbah-dry-maar-crater/ accessed on 26 August 2025]. In 2025, UNESCO accepted two nominations, Salma and North Riyadh, as UNESCO Global Geoparks [<https://www.unesco.org/en/igpp/salma-unesco-global-geopark> and <https://www.unesco.org/en/igpp/north-riyadh-unesco-global-geopark> accessed on 26 August 2025]. The Salma UNESCO Global Geopark features both a complex monogenetic volcanic field and a Neoproterozoic resurgent caldera system, illustrating diverse geological heritage [38].

This report also highlights the Lunayyir Volcanic Field near the Red Sea, identified as a Quaternary volcanic field. In 2009, volcano-seismic activity created a 20 km fissure system, with magma stopping close to the surface; although it was a failed eruption, it confirmed the area's active volcanic status and hazard potential [39–44]. Pristine volcanic landforms here serve as valuable sites for geoeducation and geotourism aimed at resilience to volcanic hazards. Western Arabia hosts at least 19 Quaternary volcanic fields, most with Late Pleistocene to Holocene eruptions, offering further opportunities for geoeducation and tourism.

Geoheritage protects the Earth's environment and benefits people, enabling them to understand their landscape, recognize hazards, and manage risks. Management comes through the identification of the geological elements (river courses, faults, volcanic rocks, etc.), placing them in a wider context, and giving them meaning and a narrative that can be used in a sustainable development strategy that includes the local community's ability to react to and absorb changes from multiple hazards. This makes the community resilient. Geoheritage is the knowledge, communication, and protection of the Earth's value to society.

Many volcanic sites, owing to their geodiversity, landscape features, and scientific relevance, can be used for projects that examine volcanic geoheritage to identify geosites suitable for geotourism, geoeducation, and geoconservation [45–50]. Identifying volcanic geosites in active volcanic regions is important because these locations serve as geological records of different volcanic hazard elements and have potential value for educational purposes related to hazard awareness and community resilience [22,26,27,51,52]. Geohazards are an important aspect of geosystem processes, especially in volcanic systems. Though research increasingly addresses hazards' interaction with geoheritage and geodiversity, it mainly focuses on preserving geosites and shielding geological features from hazards [53–57]. Most studies aim to understand these risks and protect heritage sites, but few examine geosites that directly represent volcanic hazards or record their effects [58–67]. Volcanic hazards in active systems are complex, making effective communication difficult—particularly as communities often require precise forecasts to prepare. This challenge is especially pronounced in monogenetic volcanic fields, which contain many small, short-lived volcanoes [68]; currently, it is not possible to predict when or where future eruptions will occur on a meaningful scale. In regions facing volcanic risk, uncertainty in event prediction and socio-economic consequences can drive interest in new

approaches to sustainable development. This article discusses the potential advantages of preserving important volcanic geosites for geoeducation and hazard awareness, rather than focusing only on economic measurements of volcanic hazards. While few studies exist, those that have explored these areas show that developing geoeducation and geotourism programs at volcanic sites can benefit communities and promote disaster awareness. For example, Indonesia's Toba Caldera is both a visually striking tourist destination and a model for sustainable local development involving community participation and appreciation of geotourism [69].

The geological processes responsible for the formation of Saudi Arabia's Quaternary volcanic fields have the potential to quickly alter or even eradicate these landscapes through unforeseen volcanic activity, creating significant risks to their distinctive features. Officially designated geoconservation sites, such as geoparks, play an important role in educating the public about geological phenomena and associated hazards that may impact human society. The study area discussed here is an example of the development and maintenance of geoconservation sites within a comparatively young volcanic field in Saudi Arabia. It addresses the significance of communicating geological hazards and the approaches used for mitigation and prevention. Providing clear information can support community awareness regarding geohazards, and the geoconservation site, with its selected geosites, offers educational resources on geosciences, geohazards, and risk reduction strategies. Volcanic landscapes demonstrate ongoing geological activity and attract visitors interested in geoheritage, despite the risks involved. Active volcanoes frequently reshape their environments and influence nearby communities, while less active fields, such as those in western Arabia, rarely interact with people but pose serious threats when eruptions occur. These regions enhance our understanding of volcanic hazards and offer economic benefits through geotourism, though upkeep can be expensive.

This work draws on a combination of comprehensive desktop research using available geological data, alongside field observations to verify known and potential geological features in an area being considered for tourism development within the northern Harrat Lunayyir region, part of a Pleistocene–Holocene monogenetic volcanic field [70,71]. The region is part of a broader Quaternary volcanic field regarded as active (Figure 1). Notably, recent volcanic features are characterized by a dark coloration contrast with the older, light-colored crystalline basement rocks, resulting in a distinctive landscape. This setting is under consideration for niche tourism, including adventure tourism and geotourism (Figure 1). Although Harrat Lunayyir is relatively remote (Figure 2), the area remains accessible and has been identified as suitable for slow or recreational tourism strategies. The area's young geological age, from Pleistocene to Holocene, contributes to its classification as an active volcanic field [39]. In 2009, volcano-seismic activity resulted in over 15,000 seismic events exceeding magnitude 2, leading to the relocation of approximately 40,000 residents [40–44]. This highlights the importance of incorporating volcanic hazard scenarios and mitigation assessments into development plans, especially those focused on geotourism.

This report summarizes the main geological features of northern Harrat Lunayyir, emphasizing its major rock units and structural elements. The area is under a strong development plan led by the Red Sea Global company. The development site roughly defined the core of a Quaternary volcanic field (Figure 2), while geotouristic investments were soon planned on the northern side of the volcanic field, referred to here as Option 4 area. Within this area is one of the youngest scoria cone—named here as Target Volcano—considered to be a pristine volcanic landform and proposed as a main visitation site for geotourism.

Using satellite imagery and field observations, we identified key structures such as fissures, faults, folds, shear zones, and numerous dikes, with the most detailed analysis

limited to areas targeted for future tourism. The region is characterized by Neoproterozoic crystalline and magmatic basement exposures—primarily granitoid batholiths and some layered rocks like metasediments and metavolcanics—dominated by structurally controlled hills and valleys [72,73]. Lineaments observed in terrain and satellite data confirm a strong structural influence, although few large surface faults or folds are mapped. Quaternary volcanic rocks, mainly mafic basalts from seven eruption phases (Qj, Qm1–Qm6), cover much of the area (Figure 1). The youngest units, Qm5 and Qm6, are difficult to distinguish due to limited data but are vital for assessing recent volcanic hazards. The rugged topography with narrow valley network determined by faults along horst and grabens is visible in the west-to-east topographic cross-sections (Figure 3).

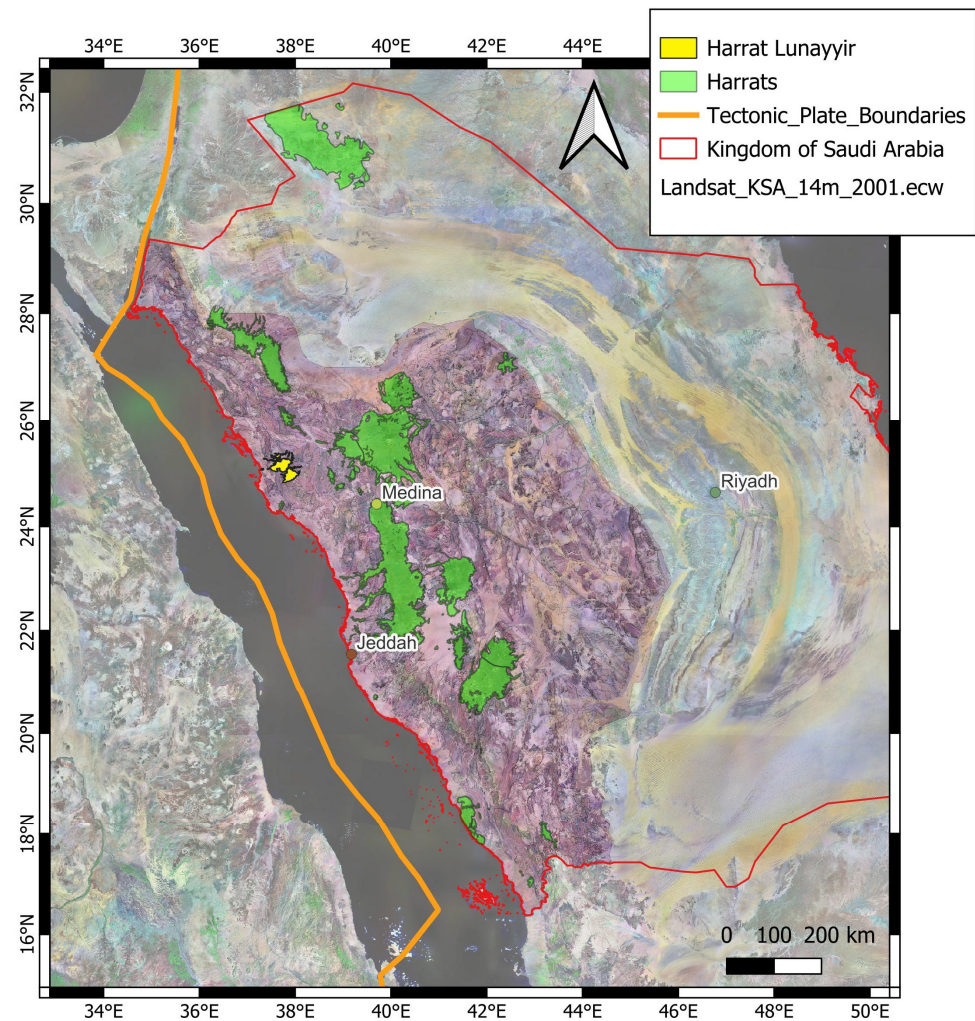


Figure 1. Harrat Lunayyir is a relatively small Quaternary monogenetic volcanic field in the western margin of the Arabian Shield composed of Neoproterozoic crystalline, metasedimentary, and ophiolitic rocks. The Arabian Shield is a structurally complex faulted composite tectonic terrain (shown with light pink on the Landsat satellite image). Quaternary monogenetic volcanic fields with extensive lava fields are significant landscape-forming elements of Western Arabia. The Red Sea Rift is the main divergent plate margin separating the Arabian Plate from Africa, connecting along transform systems in the NW margin of the Arabian Plate.

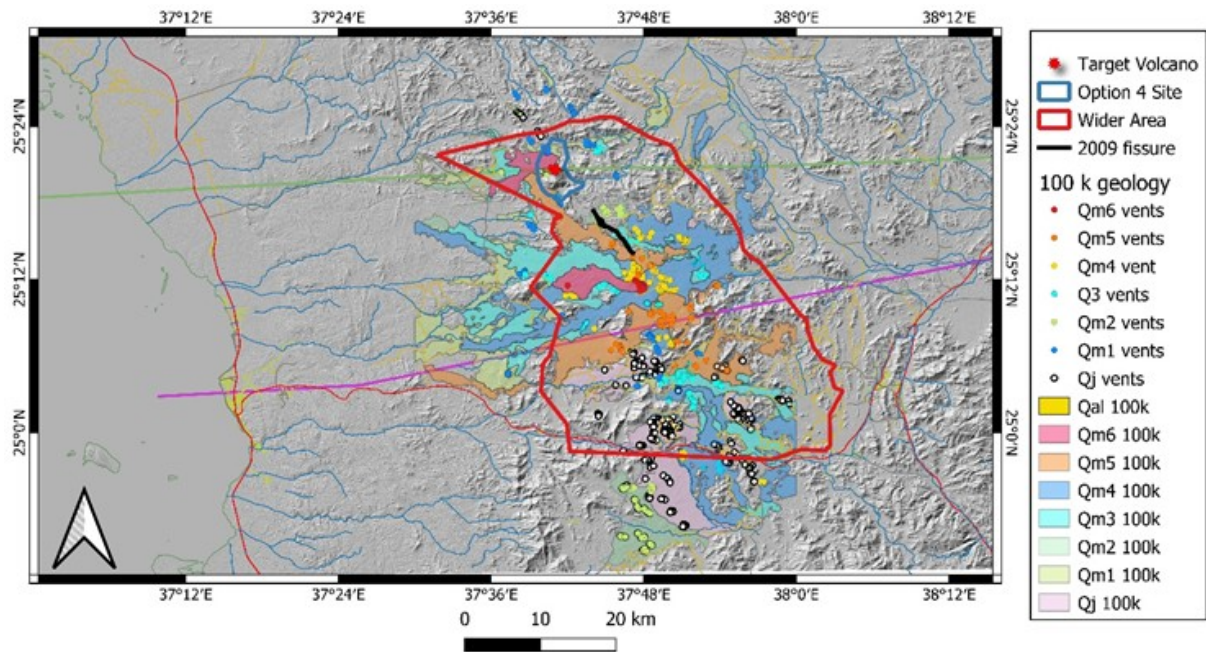


Figure 2. The map shows the lava flow-dominated regions with different color codes from the older Qj vents and Qj 100 k lava flows (around 600 ka to a suspected age of about 2.3 Ma) to the younger lava flow fields (about 500 ka to a few thousand) from Qm1 100 k to Qm6 100 k. Source vents of each lava flows are marked with Qj vents, Qm1 vents to Qm6 vents. Qal 100 k refers to the Quaternary alluvium. The Precambrian basement is forming ridge tops visible on the shaded relief map based on the 12.5 m resolution ALOS-PALSAR digital elevation data. The northern cross-section (green) and the southern cross-section (purple) are also marked on the map that is shown in Figure 3. The main target area (Option 4) is considered by Red Sea Global for tourism development, and is outlined in thick blue, while the broader area of interest in general reserve, and/or tourism development, in the long-term strategy is marked with a thick red line (Wider Area). A thick black line in the central part of the region, about 10 km SE from the Option 4 area, marks the fissure opened in 2009.

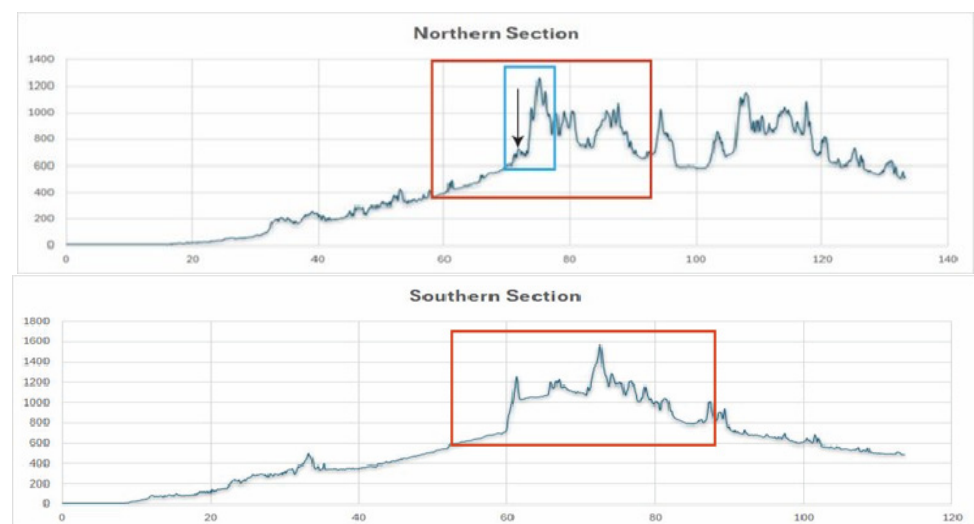


Figure 3. Cross-section across the terrain in its northern (top), southern (bottom), west (left) to the east (right) profile showing the rugged basement horst and graben structure of the region within lava flows occupying the narrow gorges. The x-axis is kilometers along the cross-section lines shown in Figure 2, while the y-axis is meters. The red box shows the area that is within the wider area of interest zone (WAI), bounded by the red line in earlier maps. The blue box shows the Option 4 region, while the arrow points to the target Volcano on the Northern Section.

This report presents map visualizations and summaries of geological features in the northern Harrat Lunayyir, based on satellite data and limited field surveys examining joint surfaces, fault planes, and shear zones relevant for regenerative tourism. It outlines the main geological structures and rock units, and identifies 26 key geosites notable for their fragility and value in geoeducation and geotourism. Most sites are essential for understanding volcanic geohazards, highlighting the region's significance in fostering community resilience through geoheritage. A comprehensive geodiversity map was also produced, combining geological and terrain elements to identify areas with high geodiversity. The research concludes that northern Harrat Lunayyir (Option 4 region of the Red Sea Global venture) is a major geodiversity hotspot, warranting inclusion in geo-conservation strategies and regenerative tourism initiatives.

2. Materials and Methods

Geoheritage, which refers to the geological component of natural and cultural heritage [74], encompasses features of geology at various scales that are considered significant for their scientific, educational, or cultural value. A geosite is an individual geological heritage asset [75], categorized similarly to other natural heritage elements such as biodiversity. Geoheritage includes features at global, national, state, and local levels that provide information about Earth's evolution, the history of science, or that have utility in research, teaching, or reference [76]. Geotourism is a form of knowledge-based tourism that integrates aspects of the tourism industry with the conservation and interpretation of abiotic natural attributes [77]. It also considers related cultural aspects within geosites for public engagement. Geodiversity describes the diversity of abiotic elements in nature, often quantified by the density of geological and geomorphological features [78–80]. This assessment involves collecting data on various geological units, minerals, soils, water sources, and parameters that objectively measure terrain morphology. In some cases, geodiversity is further assessed using a value scale based on the relative abundance and significance of specific features, such as assigning higher weights to rare rock types [80–82].

This study used remote sensing data to identify potential geosite locations in Harrat Lunayyir, with particular attention to the Option 4 region. Geosites were confirmed through geological mapping and fieldwork across four campaigns, which included reconnaissance and detailed mapping. Field descriptions of lithology and volcanological features helped establish the area's volcanic geoheritage as valuable for geohazard resilience. The main lithologies identified are briefly evaluated for their geological significance in a narrative summary.

In this context, we also used a geodiversity estimation method that identifies areas with both high feature density and higher values for educational, scientific, tourism, and conservation purposes [83]. While this approach involves uncertainties, recent evidence suggests it is an effective and efficient way to locate regions with notable geodiversity, which may indicate potential geosites [84,85]. Figure 4 provides a summary of the evaluation point system employed. Of the various terrain analysis methodologies available, our evaluation focused on terrain ruggedness (https://docs.qgis.org/3.34/en/docs/user_manual/processing_algs/qgis/rasterterrainanalysis.html, accessed on 2 September 2025), which measures variations in elevation and their relationship to neighboring units. Ruggedness is used as a proxy for landscape definition, offering additional context beyond slope angle measurements alone. For geological features, lower scores were assigned to Quaternary surficial deposits and higher scores to the youngest volcanic landforms (see Figure 4). The calculation of geodiversity for the whole region has been performed on a 2.5 km wide grid network using QGIS and its inbuilt plugins.

Main Values of Geodiversity				
Values (7-Point System)	Elements of Geodiversity			
	Geomorphology			Geology
	Slope, Roughness, Ruggedness, Total Curvature	Topographic Position Index	Geomorphon	Rock Type and Ages
1 (the lowest)	The numerical models have been included into assessment without direct evaluation.	Topographic Position Index model have been evaluated by 7-point system for positive and negative forms of landscape, where 0 is the lowest value	Flat and Slope	Alluvial, sabkha
2 (low)			Hollow and Spur	Precambrian basement
3 (low to middle)			Footslope and Shoulder	Qj volcanics (all)
4 (middle)			Valley and Ridge	Q1-2 Volcanics
5 (middle to high)			Depression and Summit	Q3 volcanics (all)
6 (high)			5-point system	Q4 volcanics (all)
7 (the highest)				Q5 volcanics (all)
8 (the rarest) Only Rocks	Q6 volcanics, including all the cones, lava flows and ash plains			

Figure 4. Geodiversity calculation value points theoretical model to apply for various morphological elements. Based on previous studies on geodiversity estimates, ruggedness turned out to be a very useful parameter that provided a very realistic geodiversity estimate; hence, here that value was used, that then combined with the known geological features.

The research relied on direct geological observations and fieldwork to verify terrain analysis data. Geosite identification was guided by local and regional geological context, site representativeness, abundance, accessibility, landscape features, and visibility—even for non-experts. Selection combined desktop studies with repeated cross-checks between the literature and field data.

The General Selection Principles of geosites (GCR), like other site-based conservation systems, is based on the idea that a country's or region's geology can be represented through select geosites (and/or geomorphosites) of special interest [10,86]. Collectively, for instance, in Wimbledon models [10,86] that were specifically developed for the United Kingdom geological site inventory; such high-quality sites capture and preserve the essence of national geological heritage. Sites were to be chosen consistently, following specific criteria and guidelines, and had to support ongoing geological research and discovery. In the UK, for the national geosite inventory builder for geoconservation, preference was given to locations with future potential rather than exhausted historical sites [10,86]. Each location carried an attribute of Sites of Special Scientific Interests (SSSIs) centered around the site's scientific values. The threshold for SSSI status was determined partly by expert judgment of a site's significance. In a territorial sense, rather than evaluating every British region, major subdivisions were based on geological criteria, mainly through dividing the geological stratigraphy column. The project used a consensus-driven approach that encouraged contributions from all stakeholders, making it a collective resource for the geological community. The Wimbledon method is foundational to many geosite recognition systems and selection theories, but its effectiveness varies in regions lacking extensive geological research or comprehensive mapping, such as Harrat Lunayyir. In these areas, consensus-based identification is challenging due to limited expert availability and often relies on initial exploratory assessments. Nevertheless, Wimbledon's core principles can guide rapid geodiversity hotspot identification by quantifying feature density and providing spatial value assessments. Identified sites may then be evaluated with established Geosite Assessment Methods covering various geoheritage aspects.

Geosites are important locations for illustrating major aspects of the country or region's geological history. In these issues, selection should identify those locations that have national significance for the geology of Saudi Arabia, or even, in a broader sense, for the

evolution of the Arabian Plate. Their significance arises from various interests across both natural and human-made environments.

Some excavated sites are noted for their research history, while others with notable features may be used for field education, which can occasionally impact key research areas. Many less visually prominent sites provide essential information for interpreting palaeoclimates, palaeogeography, ancient ecosystems, or volcanic activity [10,86]. Some significant sites have been discovered through boreholes or temporary excavations and still receive GCR status. The value of a site is determined by its interpretative potential rather than its appearance, which supports geological research and understanding. In the UK, where this concept originated, this perspective is emphasized. However, in regions with little to no prior development and early-stage land research, sites often remain undisturbed. In these situations, the intact condition of such locations should be considered, particularly if they are important for understanding geological concepts, such as eruption styles or volcano morphology, which may be relevant for assessing potential future volcanic hazards.

A comprehensive review of site coverage requires the establishment of a subject framework to systematically categorize candidate sites. Within the GCR, classification by scientific interest was prioritized, while geographical division played a secondary role. Given that the study area represents a relatively small subset of one of the youngest volcanic regions in Harrat Lunayyir, site selection also emphasized accessibility. The region's extensive and frequently impassable lava fields posed challenges for geosite identification, making it essential to consider accessible locations that best exemplify key geological concepts and scales. Consequently, geosite selection relied heavily on the assessment of accessible areas based on three principal geological aspects: (1) representative basement geology crucial for understanding early continental accretion and the formation of the Arabian Shield; (2) significant geoforms or processes preserved within the geological record of Quaternary monogenetic basalt volcanism; and (3) Quaternary surface processes, predominantly related to weathering and mass transportation. Additionally, given the area's status as a young volcanic field, our selection process also prioritized sites that clearly illustrate the major volcanic hazards associated with monogenetic intracontinental volcanism.

This work followed established Geosite Assessment Methods, particularly Brilha's approach [76,87]. A comparative study of significant geological heritage sites in Saudi Arabia internationally highlighted the region's volcanic geoheritage, supporting its value for volcanic hazard resilience education. Brilha's method for geosite evaluation has been used at several locations in Saudi Arabia, though it has not been specifically applied to volcanic regions [88–91]. This study applies the method to Harrat Lunayyir as a first comprehensive example.

3. Results

3.1. Key Geological Heritage Elements

Harrat Lunayyir (also called Harrat Al-Shaqa) is a Quaternary volcanic field with basaltic scoria cones, spatter cones, and valley lava flows. Located on the Arabian Shield, its volcanic rocks rest directly on Neoproterozoic basement rocks or thick eroded deposits.

The tectonostratigraphic units of the Arabian Shield, like other ancient continental regions, are mainly fault-bounded and have distinct geological histories [92]. These allochthonous terranes were joined through lithospheric accretion [93,94]. Due to low metamorphism and minimal surface cover, the Arabian Shield in Saudi Arabia offers exceptional exposure for studying continental accretion [94]. At Harrat Lunayyir, the well-exposed Precambrian rocks of the Shield stand out clearly against the dark Quaternary basaltic volcanic landforms. The Shield is thought to have formed during the Neoproterozoic era, over an estimated period from approximately 900 to 550 million years ago [92,94,95]. This process

produced a continental crust exceeding 40 km in thickness [94]. The current morphology and shape of the Shield are attributed primarily to more recent geological events associated with the formation of the Red Sea. Before the Red Sea opened around 25 to 30 million years ago [96], the 650,000 km² Arabian Shield was part of the larger Arabian–Nubian Shield. Today, Nubian Shield rocks are found in eastern Egypt, Eritrea, western Ethiopia, northern Somalia, and Sudan, while the Arabian Shield covers much of western Saudi Arabia with smaller exposures in the southern Levant, southern Jordan, and Yemen [97]. The Arabian Shield extends about 2200 km north–south, up to 700 km wide, with Harrat Lunayyir forming a small segment in the northwest. The Arabian–Nubian Shield is mainly juvenile crust formed by transpressive suturing between East and West Gondwana [72]. Its formation involved accretion of interoceanic island arcs along ophiolite-marked sutures between 900 and 550 Ma as the Mozambique Ocean closed [98]. An oceanic plateau from an upwelling mantle plume may also be present [99]. The area contains granitoid continental growth rocks, layered metasediments, and mafic-ultramafic complexes (ophiolites). The Arabian Shield of Saudi Arabia exhibits only minimal metamorphism, aside from localized occurrences of gneissic rocks. It represents one of the most well-preserved and extensively exposed Neoproterozoic assemblages attributable to the accretion of volcanic arcs. The shield is overlain on its eastern, northern, and southern flanks by a substantial sequence of Phanerozoic sedimentary rocks, while its western boundary is defined by the Red Sea, which presently separates the Arabian and Nubian shields. In our study, we also selected representative sections where Precambrian rocks shape the landscape and visually contrast with younger volcanic formations, providing notable aesthetic and educational value. The key geological elements of the study site can be divided into Neoproterozoic basement assemblages, Quaternary basaltic volcanic rocks, and Quaternary surface deposits.

3.1.1. Neoproterozoic Basement Rocks

The oldest rocks in the study area are Neoproterozoic, with some numeric age data available. These rocks form steep-sided horsts separated by long valleys trending NW–SE and SW–NE, likely shaped by deep structural features and shear zones between basement blocks. Mapped at a 1:250,000 scale using data from the Saudi National Geological Database (DS_250K_GM_053C sheet), the main rock types include tonalite, monzogranite, and syenogranite, which dominate the northern landscape of the investigated area.

Tonalite

Tonalite is a coarse-grained, felsic, and intrusive igneous rock composed primarily of plagioclase feldspar (usually oligoclase or andesine), with less than 10% alkali feldspar and over 20% quartz in its QAPF content. Accessory minerals include amphiboles and biotite. Unlike older definitions equating tonalite with quartz diorite, current IUGS guidelines define tonalite as having >20% quartz, while quartz diorite contains 5–20%. In the study area, two tonalite types—tn1 (more mafic, gabbroic) and tn2—have been identified, both part of the Jar Tonalite dated to 745–695 Ma. The rocks are generally light beige and intersected by mafic dikes that create distinct landscapes. Tonalites, along with granodiorites, typify calc-alkaline batholiths above subduction zones, making these sites valuable for geoeducation and geotourism by highlighting the magmatic evolution of the Arabian Shield.

Trondhjemite

Trondhjemite, a light-colored intrusive igneous rock (<https://www.mindat.org/min-51928.html>, accessed on 2 September 2025), is exposed in the NE sector of the study area. It is a tonalite variety with mainly oligoclase plagioclase. When found in oceanic crust or ophiolites, trondhjemites—often called plagiogranites—indicate oceanic crust obduction. In this study, their association with mafic layered rocks suggests they are remnants of

ancient oceanic crust, labeled 'gd' and confined to eastern surface sectors. Common in Archean terranes like the Arabian Shield, trondhjemite typically appears alongside tonalite and granodiorite as part of the TTG suite and often forms dikes within ophiolite complexes.

Monzogranit—Syenogranite

Monzogranites and syenogranites are the main crystalline basement rocks in the Option 4 area (Figure 5). Monzogranite, a plutonic rock, contains 20–60% quartz, with the rest mostly alkali feldspar and plagioclase. While monzogranite is transitional among granitoids, syenogranite resembles typical granite, distinguished by its pink hue from hematite-rich orthoclase. Syenogranite is coarse- to fine-grained, felsic, and mainly contains alkaline feldspar (usually orthoclase), 15–25% quartz, biotite, muscovite, rutile, and, occasionally, rare amphiboles (Fe-hornblende, Fe-edinite) and annite-rich biotite (25–35%). Plagioclase (An₃), K-feldspar, and quartz are also present. The central part of the Option 4 area features a prominent semicircular hill made of monzogranite from the Khanzira Complex, likely of Neoproterozoic age and slightly younger than the nearby Jar Tonalite ranges. This hill, characterized by light pinkish granite partly covered by Holocene volcanic ash, shows typical weathering with rounded blocks and fragmented material. The region contains numerous mafic dike swarms trending east–west, visible on satellite images as they curve around the central monzogranite body.



Figure 5. Neoproterozoic basement rocks (monzogranite) form the highest peaks in the Option 4 region. They are rugged, and their terrain has a complex structure. However, the rock types are monotonous crystalline basement types invaded by Neoproterozoic mafic to intermediate dikes (dark cross-cutting lines within the main mass). The highest peak coordinate is 25°20′39.43″ N, 37°41′38.30″ E. The rugged surface is covered by volcanic ash from the Qm6 Target Volcano in the right foreground.

3.1.2. Oldest Quaternary Volcanic Rock Units

Harrat Lunayyir is a monogenetic volcanic field in western Saudi Arabia, consisting mainly of small to medium scoria cones, spatter cones, and pāhoehoe lava flows. Eruptions began around 600,000 years ago. The oldest Quaternary volcanics, marked as Qj, are found in the southern perimeter but are absent in Option 4. Their features are best seen along the Umlujj–Al Ays highway, where erosion has heavily modified the lava lobes and many

source vents are unrecognizable. These ancient flows often form cascades with distinctive surface textures due to the rugged terrain. Younger volcanic rocks are mostly in the north and central areas. In Option 4, the oldest rocks belong to the Qm1 series in the north, Qm2 in the south, and Qm3 in the east (Figure 6).



Figure 6. An older scoria cone with red hue on the view (Qm1) with a welded core formed by lava spattering and composed of rheomorphic lava flows within its edifice (red layers) (location of the old scoria cone in the center right view is $25^{\circ}21'56.52''$ N, $37^{\circ}40'26.69''$ E). In the far left and right, light-colored rugged terrain composed of Neoproterozoic tonalites cross-cut by dark intermediate andesitic dikes.

3.1.3. Youngest Volcanics

The youngest volcanics in the region, formed during the Holocene, are classified as Qm5 and Qm6. These lava flows are visually similar, both displaying fresh surface textures. The volcanic cones remain intact without major gully networks, and their craters are well preserved, lacking substantial rock falls or surface deposits.

Lava Flows

Basaltic magma with low viscosity tends to produce lava flows that exhibit typical pāhoehoe surface textures. Pāhoehoe generally forms when lava has erupted at a slow rate and moves slowly over gently sloping ground [100]. In the study area, the main valley network has a low slope angle, which is suitable for pāhoehoe formation. However, pristine pāhoehoe surfaces are relatively uncommon in the field, suggesting that either the pre-eruptive landscape included characteristic steps where lava could accelerate, or the eruption rates were high during most eruptions. Both factors contributed to the prevalence of transitional lava flow types as the dominant surface textures in the study area. Pāhoehoe flows may move as sheets, within lava channels, or through lava tubes. Sheet and channel development are mainly observed along the main streamline of former lava flow paths, as documented in the youngest flow fields in Option 4. Lava tubes form when the cooled crust insulates the interior, allowing molten lava to continue moving [100–102]. Even after cooling, if lava continues to be emitted from the vent into the body of the flow, inflation can occur. Inflation and deflation features are observed in the Option 4 lava fields (Figure 7), indicating a history of emplacement by low-viscosity lava. Petrographic thin sections show

that these flows are microcrystalline and contain abundant olivine microphenocrysts and aggregates. Crystallinity increases with distance from the source due to surface cooling. Pāhoehoe flow fronts typically advance as small lobes or toes breaking out from the cooled crust [103,104], and are especially visible along the margins of extensive flow fields such as Qm5 and Qm6. Pāhoehoe surfaces are often ropy, billowing, hummocky, or smooth. Subtypes described include smooth, ropy, hummocky, shelly, slabby, spiny, toothpaste, and entrail forms. Ropy pāhoehoe, known for its distinctive appearance, forms when shear strain accumulates at the surface as flowing lava drags the cooling crust. While extensive regions of ropy pāhoehoe are rare in the Option 4 area, localized occurrences can be seen in flat areas, such as the northern edge of the Qm6 field. Shelly pāhoehoe develops in gas-rich flows where gas exsolves, creating tubes and blisters beneath thin surface crusts. This subtype is observed near the source of Qm6 flows in Option 4. Slabby pāhoehoe, characterized by jumbled plates or slabs of broken crust, represents a transition to ‘a’ā lava when the surface cannot accommodate the strain rate. It remains fluid enough to display pāhoehoe features and is common in the Option 4 area. Rubbly pāhoehoe, an even more fragmented variant, produces blocky clasts like those found in aa flows. Transitions from pāhoehoe to aa surface textures are evident in the lava fields, reflecting cooling and mechanical disruption of the crust and resulting in a rubbly succession of the flow mass [105]. The Option 4 lava fields exemplify Hawaiian-type transitional flows. Slabby pāhoehoe forms under high strain rates that approach conditions for aa, but the lava remains too fluid to fragment completely. Spiny pāhoehoe occurs under very low strain rates when the lava is crystalline and viscous, forming rough surfaces [106]; this subtype is typical in distal marginal flows in Option 4. The abundance of slabs in slabby pāhoehoe results from disruption of an initially flat pāhoehoe surface, with slabs displaying a range of brittle to ductile deformation. This disruption is usually caused by surges of lava associated with high strain rates, particularly in large, sheet-like lobes. In Hawaii, slabby pāhoehoe rarely extends beyond a kilometer before transitioning to classic aa or reverting to pāhoehoe if the flow rate decreases. At Option 4, the Qm6 lava flows demonstrate similar relationships between distance and surface texture.

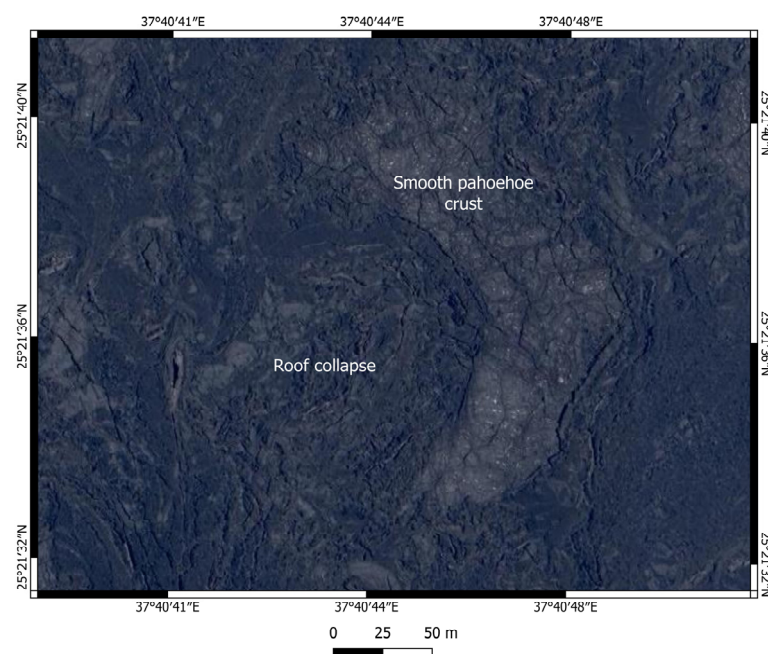


Figure 7. Roof collapse features a young lava flow in the northern Harrat Lunayyir.

Ash Plain

A defining feature of the Option 4 region is its extensive ash plain (Figure 8), formed by explosive mafic volcanic eruptions, likely originating from the Target Volcano based on pyroclast distribution and composition. The ash plain consists of coarse-grained, lapilli-sized material near the source, transitioning to finer ash farther away. Proximal pyroclasts exhibit a bluish tint due to high-temperature titanium minerals and are highly vesicular, making them lightweight and capable of traveling great distances. These low-density particles are easily eroded from peaks and contribute fine ash to alluvial systems, indicating widespread ash coverage up to 10 km from the vents. The north–northwestward spread and estimated plume height of up to 10 km suggest sub-Plinian eruptions like Parícutin, Mexico [107,108]. Microscopically, ash and lapilli display glassy, sharp-edged textures and irregular vesicles, posing potential health risks if inhaled or if entering cooling systems. Their high surface area allows the absorption of chemicals, increasing hazard potential during eruptions. Accumulated ash mixed with local dust can be re-released by activities like excavation or driving, raising concerns about carcinogenic zeolites such as erionite [109]. The region also contains scoria cones and numerous degassed lava bombs and blocks—often spindle-shaped due to ballistic transport—with compositions typical of basaltic rocks rich in plagioclase microlites and olivine microphenocrysts.



Figure 8. Ash blanketed region in the NW side of the target volcano at the GS20 geosite (25°20′44.63″ N, 37°40′38.70″ E). Note the reddish ash is oxidized scoria resulting from proximal emission and, hence, is likely marking the location of localized fire pits (vents). Most of the ash is dark, with bluish iridescence suggesting high temperature titanium mineral formation. The area is a very fragile region, and strong restrictive rules need to be enforced as uncontrolled wandering around the ash plain is not just visually damaging it, but also footprints can act as erosional initiation points for next intensive rainfall or wind actions.

3.1.4. Quaternary Surficial Sediments

The Option 4 area and its surroundings contain significant Quaternary surficial deposits, including alluvial fans, valley-filling sediments, and sabkha deposits that have accumulated in closed, temporary shallow lakes. These deposits consist of particles from nearby crystalline basement rocks, various basaltic volcanic materials, and fine-grained aeolian silts with locally occurring salt and zeolite minerals. Nearby valley networks adjacent to the crystalline basement are filled with light-colored sand and silt, while areas close to the former ash-covered ridges contain black reworked ash.

3.2. Geodiversity of Harrat Lunayyir

Geodiversity mapping shows that areas with steep, rugged terrain and young volcanics—highlighted in dark red in Figure 9—have the highest geodiversity. Comparisons with basement, Qm5, and Qm6 volcanics reveal that Option 4 represents a significant geodiversity hotspot with many valuable geosites.

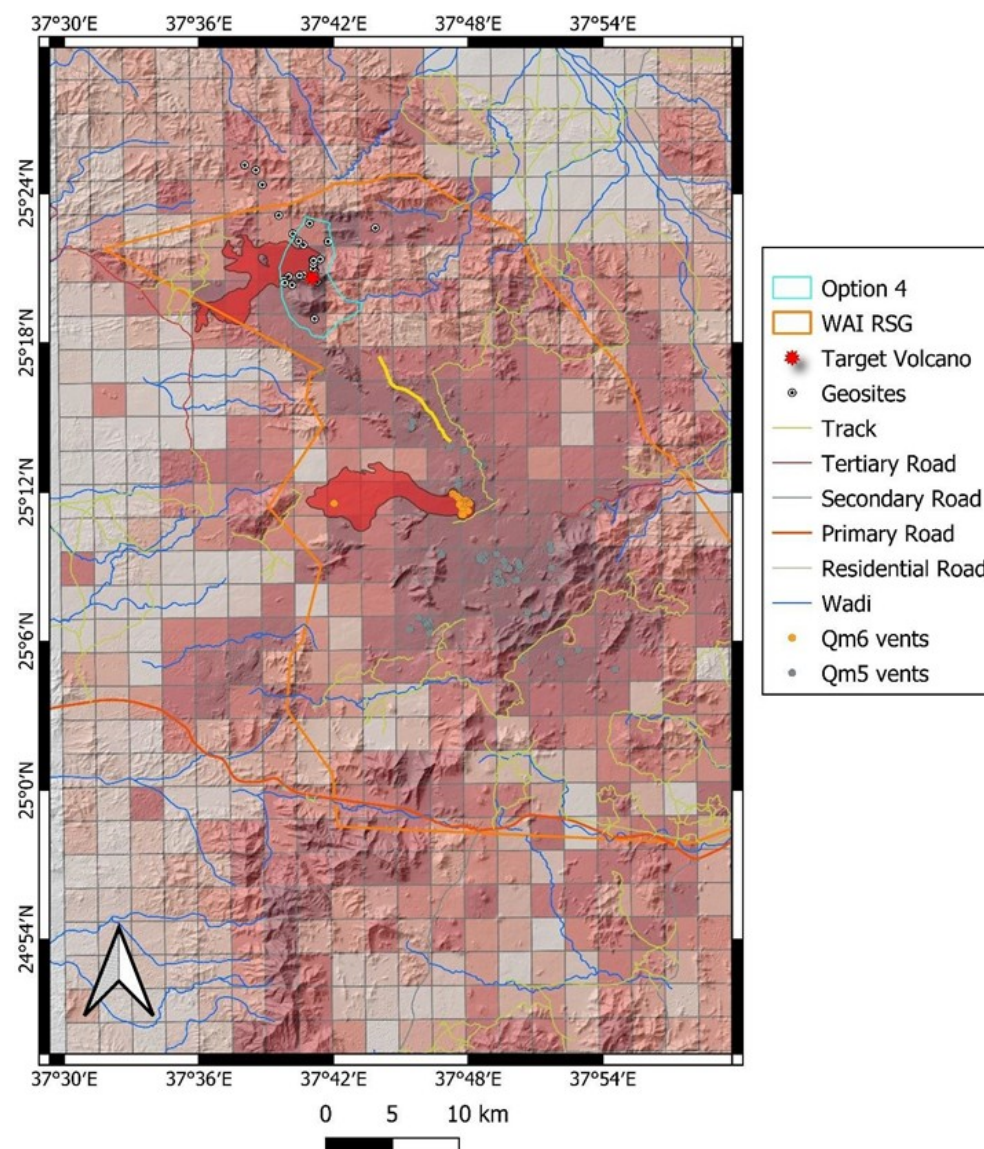


Figure 9. Geodiversity distribution and location of the youngest lava flows in the area. Note that the area of Option 4 falls into the highest geodiversity value area and the boundary of the project site well represents the region's highest valued geological sites; hence, the site selection should also be included in the geoconservation strategy. The geodiversity values were classified into simple relative categories, such as low to high, and represented in a color scheme from light-to-dark red tones. The deeper the red, the higher the geodiversity calculated and shown on the map. The two youngest lava flows are marked with a bright red color. The bright yellow line represents a fissure opened during the 2009 seismic crisis of the region. (WAI RSG—wider area of interest for tourism development by the Red Sea Global).

3.3. Geosite Recognition for Northern Harrat Lunayyir

Geosites are distinctive locations with notable geological or geomorphological features within a given area. The most valuable geosites are those recognized at regional or global levels. Their identification relies on understanding local geology and geomorphology—here, specifically in the Option 4 area—using a transdisciplinary approach. Based on our prior studies, we identified 26 geosites in this region (Figure 10), which are briefly described with both textual and visual information. Table 1 summarizes these sites and their geographic locations.

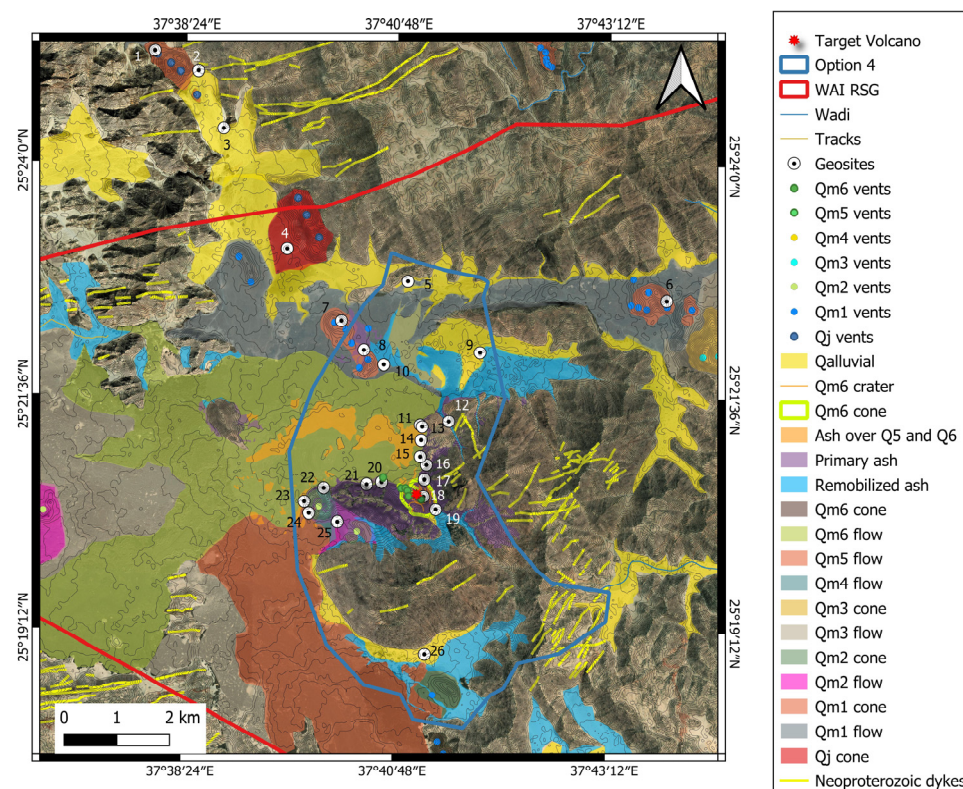


Figure 10. Identified geosites (with their code numbers listed in Table 1) in the northern Harrat Lunayyir. The map shows the various lava flows and vents ordered in their stratigraphy position. Where the satellite image is not covered by colored pattern represents exposed Neoproterozoic basement rocks. Primary and remobilized Holocene volcanic ash form an extensive sedimentary cover over the rugged landscape. The background is a Bing satellite image and topography enhanced by 10 m density contour lines derived from the ALOS-PALSAR digital elevation data.

Table 1. Geosite inventory for the Option 4 area: Significance is assessed as local, regional, or global. Local sites are unique within the area but common regionally, regional sites are rare in the region with notable preservation or appearance, and global sites are considered reference points or unique features on a worldwide scale. The decision to determine each site to be ranked as local, regional, or global is based on expert opinion, the common scientific literature data, and the geological context of the site. Bold, underlined geosites in a cream color row are locations where volcanic geoheritage of the Quaternary volcanic field is exceptionally well preserved and demonstrated.

Geosite Code	Lat	Long	Description	Significance
<u>GS1</u>	25°25′8.61″ N	37°38′2.32″ E	Eroded scoria cone and associated lava field. Archeology sites are on top of the lava flow.	Local but archeology sites can be global
GS2	25°24′56.29″ N	37°38′31.62″ E	Dark massive dike in meters wide crosscutting the light-colored tonalite crystalline rocks.	Local to Regional
GS3	25°24′20.87″ N	37°38′49.57″ E	Archeological site made from dike fragments derived from a nearby mafic to intermediate dike.	Regional to Global
<u>GS4</u>	25°23′14.52″ N	37°39′33.16″ E	Welded scoria core and agglutinate preserved on steep basement horst, potentially along a fault.	Regional
<u>GS5</u>	25°22′47.30″ N	37°40′54.37″ E	Former lava flow level mark.	Local to Regional
<u>GS6</u>	25°22′29.84″ N	37°44′0.93″ E	Quarried scoria cone with extensive ash and lapilli beds; perfect exposures to see the internal architecture of scoria cone complexes.	Regional

Table 1. Cont.

Geosite Code	Lat	Long	Description	Significance
GS7	25°22'23.06" N	37°40'7.01" E	Qm1 stage scoria cone in well-preserved condition with ash cover.	Regional
GS8	25°21'58.45" N	37°40'26.68" E	Agglomerate proximal scoria cone core and open crater that is accessible. Lee side ash accumulation in wind shadows.	Regional
GS9	25°21'56.03" N	37°41'36.63" E	Sabkha deposit, silt pan.	Local
GS10	25°21'53.55" N	37°40'41.22" E	Pahoehoe lava flow margin with inflation and deflation features.	Local
GS11	25°21'19.98" N	37°41'5.08" E	Spectacular slabby pāhoehoe lava surface texture.	Regional to Global
GS12	25°21'22.03" N	37°41'24.14" E	Complex volcanoclastic fan deposit with recent gravity flows and rock falls.	Regional to Global
GS13	25°21'18.34" N	37°41'5.31" E	Monzogranite as a main rock type of the high ranges behind the Target Volcano.	Local
GS14	25°21'10.99" N	37°41'7.24" E	Flow lobe tumuli.	Local to Regional
GS15	25°21'0.52" N	37°41'5.20" E	Slabby pāhoehoe lava flow margin.	Local to Regional
GS16	25°20'54.72" N	37°41'9.32" E	Scoriaceous ash and lapilli-dominated fan.	Regional
GS17	25°20'46.31" N	37°41'8.23" E	Ballistic bomb field.	Regional to Global
GS18	25°20'35.74" N	37°41'6.55" E	Complex crater of the youngest volcano in the region.	Regional to Global
GS19	25°20'27.72" N	37°41'16.09" E	Small intramountain basin with complex volcanoclastic sedimentary infill.	Regional to Global
GS20	25°20'44.63" N	37°40'38.70" E	Ash plain covering the landscape.	Regional
GS21	25°20'43.93" N	37°40'26.06" E	Partially ash-covered aa lava flow.	Regional
GS22	25°20'40.90" N	37°39'59.23" E	Series of gullies covered by primary volcanic ash and lapilli.	Regional
GS23	25°20'32.28" N	37°39'46.08" E	Preserved primary ash fall in thick successions.	Regional
GS24	25°20'23.59" N	37°39'48.18" E	Convulsion of various lava flows entering an open-crater old scoria cone.	Regional
GS25	25°20'20.92" N	37°40'12.24" E	Complex volcanoclastic sedimentary fan.	Regional
GS26	25°19'2.88" N	37°41'33.06" E	Ash starved alluvial fan in a closed basin.	Local

Each of these sites can serve as a destination within both self-guided and organized tours, and may be incorporated into geotrails—a widely adopted approach in geotourism development globally [110–114]. Geosites may subsequently be assessed using standardized and internationally recognized criteria [76,87]. Initially, we provide detailed descriptions of geosites and then present an evaluation to substantiate the rationale behind their selection. For clarity, the areas have been subdivided into smaller regions to better illustrate the comprehensive geological insights these locations offer to visitors.

The northernmost region, situated just outside Option 4 territory yet near it, comprises a complex system of older scoria and spatter cones occupying a relatively small valley within the Neoproterozoic basement. Geosites are designated as GS with numbers ranging from 1 to 26. GS1 features a scoria cone complex from an ancient volcano that retains relatively well-preserved geomorphology despite noticeable erosion (Figure 11). This site provides valuable insights into advanced stages of erosion over several hundred thousand years, serving as a useful comparison to younger volcanic geosites (Figure 12). The nearby Neoproterozoic basement is intersected by mafic dike swarms, offering convenient opportunities to observe and examine these rocks firsthand at GS2. At the entrance to this valley network lies an archeological site marked by circular stone formations on the desert floor, making it one of the most accessible and intricate geoarchaeological locations within the wider area of interest (Figure 13).

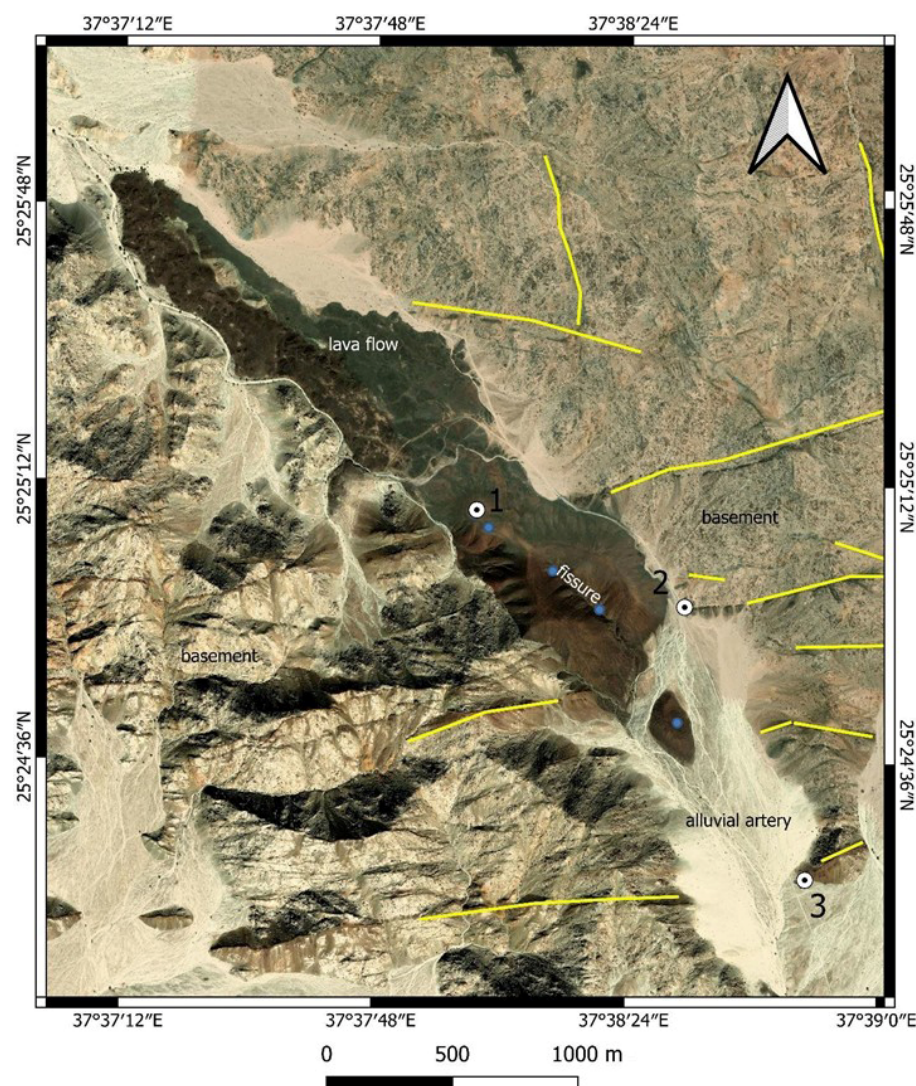


Figure 11. Close-up view (Bing Satellite Imagery) of the Geosite 1, 2, and 3. The area is outside of the Option 4 region, but, as it is a confined, intact older volcanic region formed in a narrow valley in addition to its high aesthetic values, it demonstrates a geological process so typical in Harrat Lunayyir; namely, the narrow value-captured monogenetic volcanism. GS1 is a lookout point on top of an older scoria cone. GS2 is a Neoproterozoic dike edge. Dikes are marked with yellow lines (only the representative ones). GS3 is an archeological site where basement rocks formed some sort of circular feature with an unknown purpose.



Figure 12. GS1 geosite ($25^{\circ}25'8.61''$ N, $37^{\circ}38'2.32''$ E) of an old scoria cone and associated lava flow filling the longitudinal valley. On the lava surface, archeological sites are well preserved as keyholes and long arrows like stone arrangements.



Figure 13. Archeological site formed by crystalline basement of Jar tonalite and Neoproterozoic dike rocks on the alluvial plain is the GS3 geosite (25°24′20.87″ N, 37°38′49.57″ E). Note the dikes in the background range forming edges of darker colored rocks through the tonalite.

Superb geosites are found along the northern edge of Option 4's main access road, showcasing older scoria cones and lava flow margins (Figure 14). GS4 is a prime example in the study area, illustrating how scoria cones develop over rugged terrain (Figure 15). The agglutinated lava spatter core of the scoria cone forms an erosion-resistant center that preserves the Neoproterozoic basement below.

The preservation of a scoria cone in steep, rugged terrain is an uncommon occurrence; this geosite allows visitors to consider the primary factors influencing cone growth and its preservation. This location is not only relevant within the study area but also holds global significance for research in volcanology.

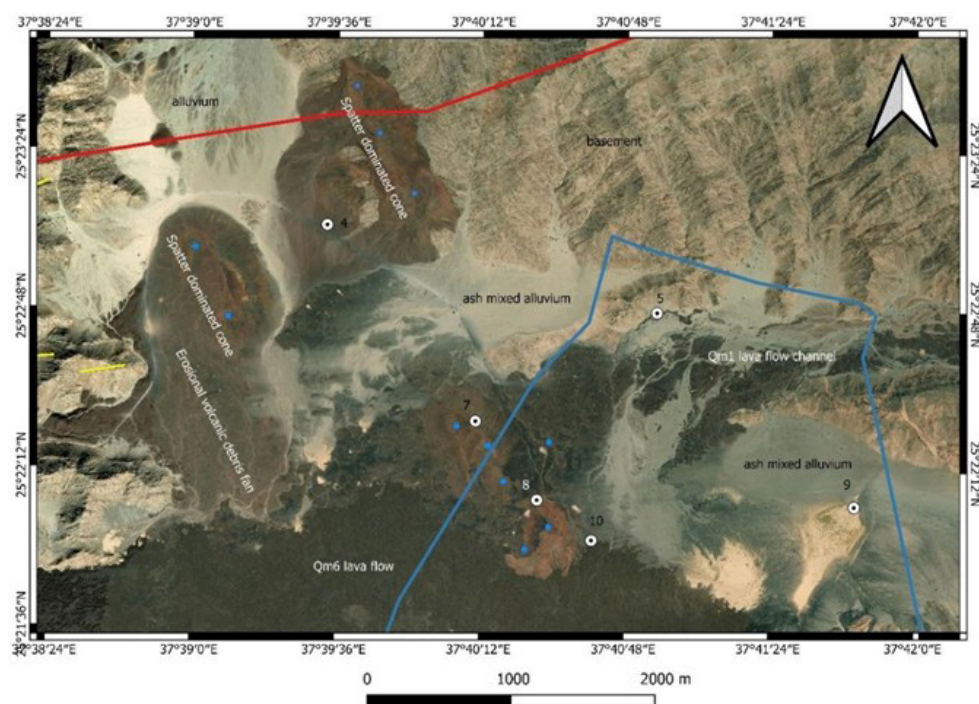


Figure 14. Geosites map in the northern edge of Option 4 region. GS4 is an old scoria cone built on the steep slope of the basement due to lava spattering, while GS7 and GS8 are part of similar scoria cones formed on a flat surface. GS5 and GS10 are lava flow features. GS5 is a typical high stand marker of preserved lava representing the highest level of lava inundation before lava drained from the region, while GS10 is a typical pāhoehoe lava flow edge of the youngest flow of the region. GS9 is a complex sedimentary environment where aeolian, alluvial, and sabkha deposits are mixed with fine ash.



Figure 15. GS4 geosite ($25^{\circ}23'14.52''$ N, $37^{\circ}39'33.16''$ E) is a spectacular scoria cone (dark draping rocks over light-color basement rocks) from the Qm1 stage that erupted on a steep, and probably fault-bounded, terrain. Basement rocks of Jar tonalite (light) crop out from the gradually stripped scoria surface. The background of the ridge is composed of slightly more mafic tonalite.

GS7 is a geosite that preserves a Qm1 scoria cone (Figure 16) with considerable integrity. The outer flank of the cone shows well-developed gully systems, suggesting the cone existed during pluvial periods when these features gradually formed on its sides. Despite the gullies, the volcano's original shape remains largely intact, including a preserved crater and rim attributed to the welded pyroclastic collar at the crater lip. These characteristics suggest that the volcano is relatively young and corresponds to models of scoria cone degradation and morphometry, indicating that a volcano less than a million years old would be expected to have similar features [115–122].



Figure 16. GS7 ($25^{\circ}22'23.06''$ N, $37^{\circ}40'7.01''$ E) is a Qm1 stage scoria cone where a gully network developed, indicating its formation before major pluvial periods. The cone is conical in shape, but its crater is clearly preserved by spatter ramparts, and the outer flanks are already erosionally modified. Note the slightly reddish Target Volcano cone in front of the basement crystalline rock cliffs partially covered by ash.

GS8 is a location that connects well to the GS7, as easy access to the former crater of a scoria cone reveals the densely welded nature of the preserved pyroclasts, forming a castle-like skeleton of the former volcano, and keeping the core of the volcano preserved. Just next to the GS8 cone, the young Qm6 lava flow reaches a region blocked by the GS7 scoria cone, demonstrating interesting interaction features of slabby pāhoehoe lava flow margin development. At GS8, deflation and inflation features can be observed, indicating typical pāhoehoe lava flow evolution stages that make this geosite unique within the Option 4 area.

The lava flow margin features are prominent within the study area. GS5 serves as an example, illustrating that the original lava infill was elevated within the longitudinal valley network adjacent to the Option 4 territory. This geosite allows for observation of large-scale lava flow behavior within confined environments such as a narrow valley network.

GS9 is a sabkha situated within a closed basin formed by multiple lava flows. These regions are located near the elevated peaks of the basement, where runoff water gathers and forms temporary lakes. The silts present in the lake beds can become sources of dust when strong winds occur.

Situated slightly apart from Option 4, there is an older, complex scoria cone designated as a geosite due to its distinctive structural characteristics (Figure 17). This scoria cone complex developed within a locally open area at the intersection of narrow valleys (Figure 18), resulting in the formation of an amalgamated system with overlapping volcanic edifices. The intricate architecture of the site is exposed by local quarrying activities, which allow access to various types of scoria layers. Within the quarry, large, degassed volcanic bombs and blocks are present, serving as evidence that active craters periodically accumulated molten material, which solidified before being expelled as clasts during subsequent eruptive events.

Visitors can access the interior of the area via a walking path originating from the main 4WD road (Option 4). The terminus of the 4WD track marks an ideal geosite (G12), distinguished as one of the largest debris fans accumulating eroded ash and lapilli from the monzogranitic hilltops. As one approaches the Target Volcano, the footpath traces the boundary between the Qm6 lava flows, alluvial fans, and the principal basement horsts. GS13 provides optimal exposure to the monzogranite basement due to its accessibility. Additional geosites, including GS11, GS14, and GS15, illustrate various features of slabby pāhoehoe lava flow margins. GS16 represents a primary ash-dominated fan.

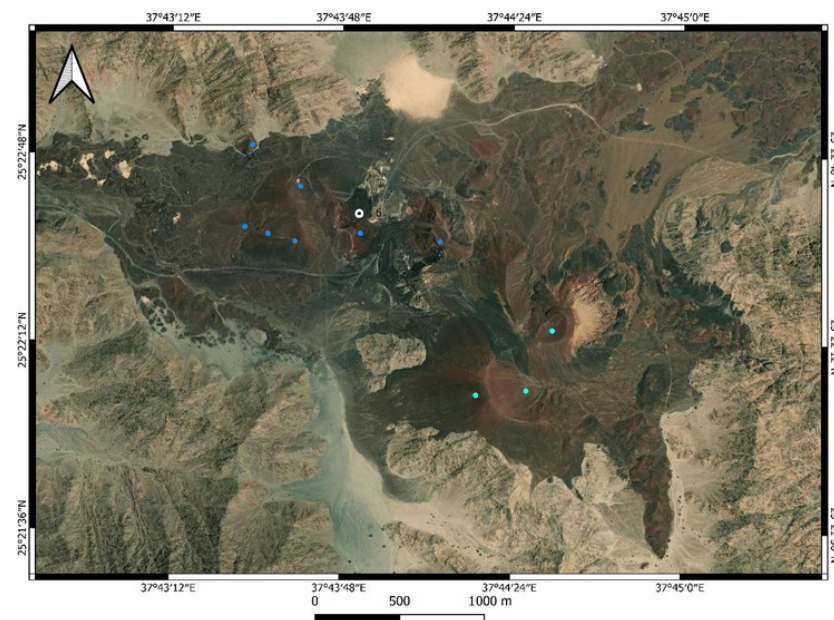


Figure 17. GS6 geosite ($25^{\circ}22'29.84''$ N, $37^{\circ}44'0.93''$ E) is the most representative location of a very complex scoria cone complex that is outside the Option 4 territory. It is an active quarry where quarry walls perfectly expose the proximal sections of compound scoria cones formed over a long time and very likely in different evolutionary stages. The volcanic complex formed in the juxtaposed location of three types of basement rocks. In the SW edge of the region Jar tonalite, in the northern and eastern side of the volcanic complex, Fara' trondhjemite forms the exposed basement rocks surrounding the volcanic complex. Blue dots represent Qm1, while green dots Qm3 vent locations.



Figure 18. Volcanic complex of amalgamated scoria cones GS6 ($25^{\circ}22'29.84''$ N, $37^{\circ}44'0.93''$ E) from the west fills the morphological depression within the basement horst. The light-color rocks of the ridge on the left side of the view are part of the mafic Jar tonalite.

Upon reaching the Target Volcano (Figure 19), the GS17 region is characterized by numerous volcanic bombs scattered across a recently deposited ash plain, illustrating the dominant path of ballistically ejected material from the nearby primary vent. This area is extremely fragile and should be subject to stringent conservation measures. Most bombs remain within their respective impact craters, highlighting the eruption's recent occurrence.

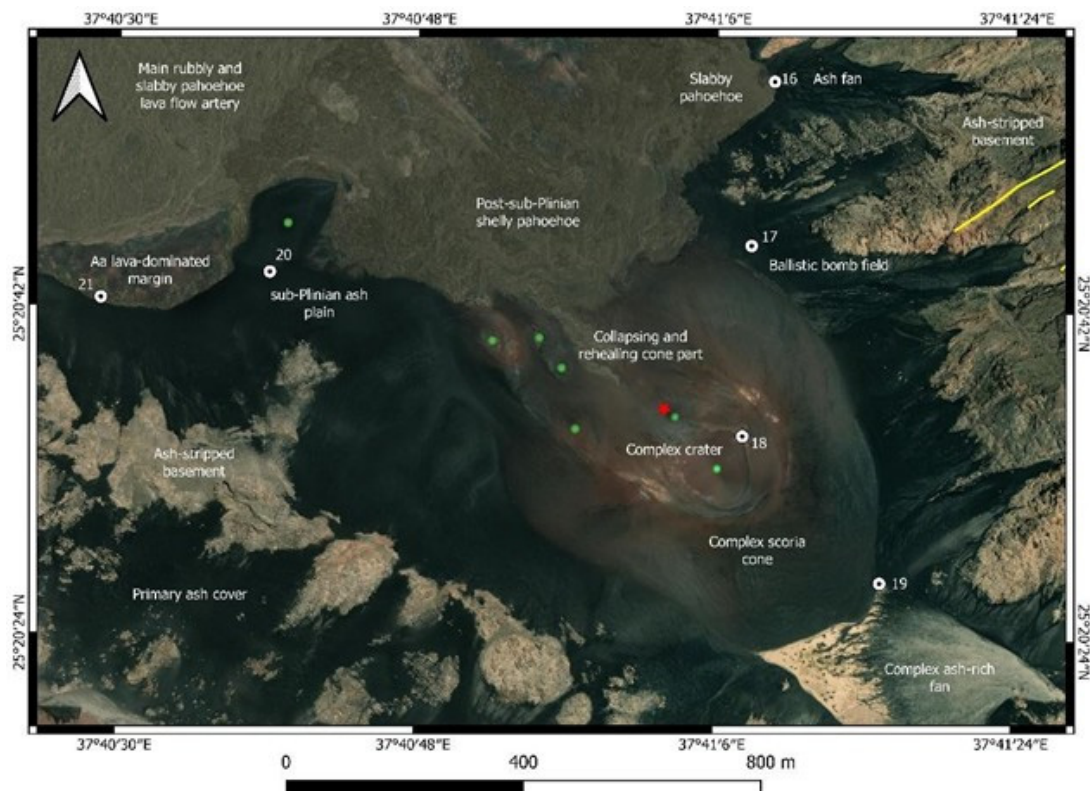


Figure 19. Overview geological sketch map based on Bing satellite imagery from the center area of the Option 4 region. This area records volcanic features associated with the scoria cone growth, and its explosive and effusive as well as collapsing stages. These geosites are very fragile, and proper geoconservation strategies are recommended to be developed to keep the integrity of the area intact. The image also demonstrates that the Target Volcano (red star) is a complex and potentially active (weeks to months) volcano, judging from its size and complex crater morphology. Narrow ridges along its crater indicate gradual step-like collapses toward NW. Each of the collapses or gradual spreading is inferred to be the result of lava flow emission from the crater toward the NW, letting the crater floor sink, and, through explosive phases, re-heal. The latest lava flow that came from the crater is not covered by ash (marked as post-sub-Plinian rubbly pahoehoe), while, in the western areas, aa-

type lava is covered with ash. This indicates that the volcano went through stages of eruptions when explosive phases were accompanied by lava flow emission that lasted well after the explosive phases resumed, leaving behind a complex flow channel network within the main Qm6 lava flow field. Identified Qm6 vents are marked by green dots.

GS18 designates the geosite at the main volcanic cone itself. The cone exhibits steep, challenging terrain that requires careful access to minimize the risk of accidents and prevent the formation of artificial gullies that may compromise its structural integrity. The crater displays a complex morphology, indicative of multiple episodes of collapse, spreading, and subsequent healing.

On the northeast flank of the cone lies a notable closed basin, providing an exemplary site for observing arid sedimentation processes (Figure 19). Here, flash flood deposits, rockfall debris, and sheetwash sediments accumulate, progressively filling a narrow valley less than one kilometer wide (Figure 19). In the western sector of the central cone, an undisturbed ash plain remains preserved, representing a highly sensitive environment where access should be strictly regulated (Figure 20).



Figure 20. The eastern side of the Target Volcano represents a typical intramountain basin at GS19 (25°20'27.72" N, 37°41'16.09" E) where primary ash and lapilli accumulated and are partially re-worked due to sheet wash erosion. The eastern side of the Target Volcano is surrounded by a monzogranite and syenogranite complex (light-color rocks in the background). This basement ridge was partially blanketed by dark scoriaceous ash that was gradually stripped away since the volcanism ceased. This geosite is a very fragile region, and restricted access is recommended, as footprints and tire tracks can damage the integrity of the area.

Pioneer vegetation is starting to colonize the area, highlighting the geo-ecosystem's fragility (Figure 20). Westward, at the edge of the Qm6 lava flows, cooling and crystallization have led to spiny pāhoehoe to 'a'ā lava transitions, resulting in unique rock formations that distinguish GS21 as a notable geosite (Figure 21). The most remote part of Option 4 features a complex geotope with five distinct geosites (Figure 22), where two Qm2 scoria cones are surrounded by Qm5 and Qm6 lava flows, creating a striking landscape. These old cones have well-developed gully networks in ash and lapilli deposits, forming striking black gullies. Like GS22 (Figure 23), the ash base can be accessed via gullies, which is crucial for studying initial explosive eruption deposits and understanding the volcano's eruption

mechanisms. On the west side of the Qm2 cone, over 2 m of primary pyroclastic succession remains preserved (GS23), showing about a dozen layers that indicate multiple explosive eruption events. In the western edge of the Qm2 scoria cone at GS24 and GS25, a spectacular view shows the complex interaction between cones; ash falls and young lava flows.



Figure 21. Another view of the GS21 ($25^{\circ}20'43.93''$ N, $37^{\circ}40'26.06''$ E) with a fantastic squeeze-up feature on the aa lava margin. In the background, the monzogranite basement horst that is partially covered by ash is clearly visible. Note the reddish ash regions marking localized, short-lived vents that emitted ash during the explosive phase of the volcano growth.

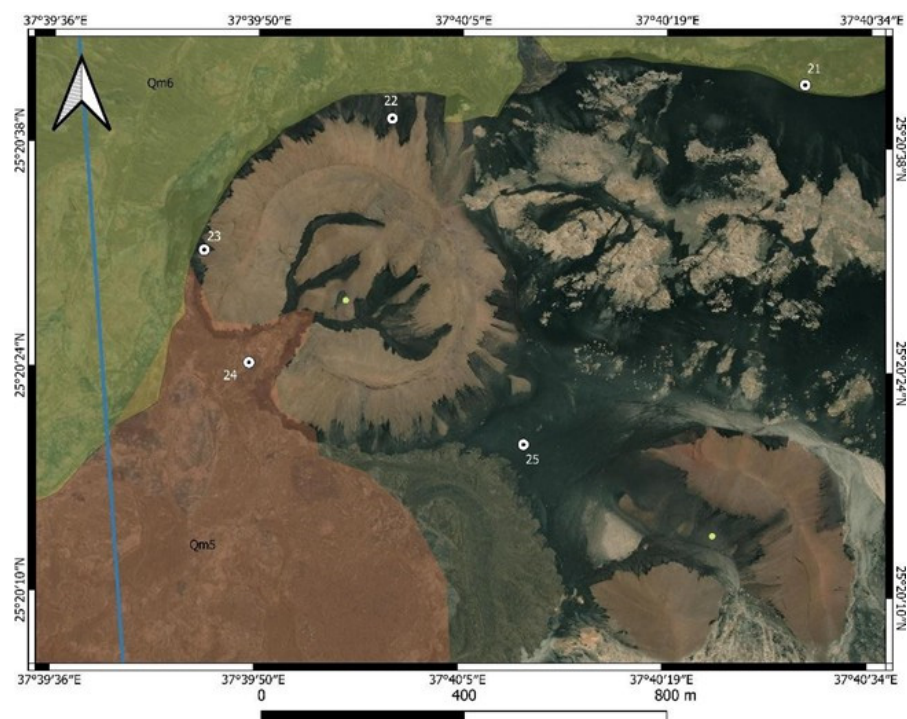


Figure 22. The most remote side of the Option 4 area exhibits a complex region where older Qm2 volcanoes are partially covered by ash (black areas) derived from the region of the Target Volcano (Qm6)

and the two youngest flow fields (Qm5—light brown field—and Qm6—light green field) meet. The identified geosites are very important messengers of the geological history; hence, their preservation is very important for future research. The blue line represents the Option 4 development area's western margin.



Figure 23. Ash covered gullies at GS22 (25°20'40.90" N, 37°39'59.23" E). Note the ash cover on the aa lava margin, indicating that following the ash emission, lava flow outpouring was still ongoing.

3.4. Geosite Assessment from a Global Perspective

Identified geosites are typically evaluated against international standards. One widely endorsed approach is the Brillha method [87], which assesses geosites based on expert evaluation from scientific, educational, touristic, and degradation risk perspectives. Although this methodology was originally designed with geoeducation and geotourism in mind—primarily within developed regions—its evaluation criteria often reflect priorities that may not be entirely applicable to remote areas such as Harrat Lunayyir. Despite these limitations, we applied this framework and obtained noteworthy results (see Tables 2–5), indicating that the nominated geosites possess significant value and uniqueness.

The 26 geosites identified demonstrated strong performance in the scientific value assessment using Brillha's method (Table 2). In this evaluation, the lowest scores for each geosite were attributed to the key location and scientific value categories, reflecting the limited direct scientific research conducted at these sites—primarily due to their remote locations. Additionally, many of the sites are considered non-unique within the regional context, as similar volcanic geoheritage features are prevalent across the Quaternary volcanic fields of Saudi Arabia. Nonetheless, the high scientific value of most of these geosites is attributed to their well-preserved landforms, clearly representative features, and significant potential for use in volcanic hazard education.

The Potential Touristic Use (PTU) (Table 3) assessment indicates that the 26 identified geosites possess tourism potential. However, effective planning is necessary to minimize possible long-term impacts associated with development in the area. At the same time, certain development initiatives may be required to address regional access issues and responsibly utilize the area's touristic opportunities, which could involve regeneration-, adventure-, or nature-based tourism for limited visitor numbers.

Table 2. Scientific value matrix of the identified geosites in the region around the area of Option 4. Each category was assigned with 1, 2, or 4 points, representing the geosite values. The greater the value, the higher the points were. Weight classes are used to calculate the overall value of the geosite listed in the left side of the table.

Scientific Values	Weight	Geosites	Representativeness	Key Locality	Scientific Knowledge	Integrity	Geological Diversity	Rarity	Use Limitations	Total Weighted
<i>Representativeness</i>	30	GS1	2	1	1	4	2	1	4	2.1
<i>Key Locality</i>	20	GS2	2	1	1	4	1	1	4	2.05
<i>Scientific knowledge</i>	5	GS3	2	1	1	4	1	2	4	2.2
<i>Integrity</i>	15	GS4	4	1	1	4	4	4	4	3.25
<i>Geological diversity</i>	5	GS5	2	1	1	4	1	2	4	2.2
<i>Rarity</i>	15	GS6	4	1	1	2	4	2	4	2.65
<i>Use limitations</i>	10	GS7	2	1	1	4	4	2	4	2.35
<i>Total</i>	100	GS8	2	1	1	4	2	2	4	2.25
		GS9	2	1	1	2	1	1	4	1.75
		GS10	2	1	1	4	2	1	4	2.1
		GS11	2	1	1	4	1	2	4	2.2
		GS12	4	1	1	4	2	2	4	2.85
		GS13	2	1	1	4	1	1	4	2.05
		GS14	2	1	1	4	1	1	4	2.05
		GS15	2	1	1	4	1	1	4	2.05
		GS16	4	1	1	4	2	4	4	3.15
		GS17	4	1	1	4	2	4	4	3.15
		GS18	4	1	1	4	4	2	4	2.95
		GS19	4	1	1	4	4	2	4	2.95
		GS20	4	1	1	4	2	4	4	3.15
		GS21	4	1	1	4	2	2	4	2.85
		GS22	2	1	1	4	2	2	4	2.25
		GS23	4	1	1	4	2	4	4	3.15
		GS24	4	1	1	4	4	2	4	2.95
		GS25	4	1	1	4	2	2	4	2.85
		GS26	2	1	1	4	2	1	4	2.1

Table 3. Potential Touristic Use (PTU) matrix of the geosites in the region around the area of Option 4. The PTU values are also calculated at 1.2 and 4 points and represent the location's increasing values. The wight values for the total PTU calculation are given on the left side of the table.

PTU	Weight	Geosites	Vulnerability	Accessibility	Use Limitations	Safety	Logistics	Density Population	Association with Other Values	Scenery	Uniqueness	Observation Conditions	Interpretative Potential	Economic Level	Proximity to Recreational Areas	Total Weighted
<i>Vulnerability</i>	10	GS1	4	1	4	1	2	1	4	2	2	4	4	1	1	2.35
<i>Accessibility</i>	10	GS2	4	1	4	1	2	1	4	2	2	4	4	1	1	2.35
<i>Use limitations</i>	5	GS3	3	1	4	1	2	1	4	3	4	4	4	1	1	2.6
<i>Safety</i>	10	GS4	4	1	4	1	2	1	3	4	4	4	4	1	1	2.8
<i>Logistics</i>	5	GS5	2	1	4	1	2	1	2	1	3	4	4	1	1	2
<i>Density population</i>	5	GS6	1	1	4	1	2	1	4	2	3	2	4	1	1	2.05
<i>Other values</i>	5	GS7	4	1	4	1	2	1	4	4	2	4	4	1	1	2.65

Table 3. Cont.

PTU	Weight	Geosites	Vulnerability	Accessibility	Use Limitations	Safety	Logistics	Density Population	Association with Other Values	Scenery	Uniqueness	Observation Conditions	Interpretative Potential	Economic Level	Proximity to Recreational Areas	Total Weighted
Scenery	15	GS8	3	1	4	1	2	1	2	3	3	4	4	1	1	2.4
Uniqueness	10	GS9	1	1	4	1	2	1	2	1	1	2	2	1	1	1.4
Observation conditions	5	GS10	3	1	4	1	2	1	2	3	2	4	4	1	1	2.3
Interpretative potential	10	GS11	2	1	4	1	2	1	2	2	4	4	4	1	1	2.25
Economic level	5	GS12	1	1	4	1	2	1	4	4	3	4	4	1	1	2.45
Proximity to recreational areas	5	GS13	3	1	4	1	2	1	4	3	1	4	3	1	1	2.2
Total	100	GS14	3	1	4	1	2	1	3	3	3	4	4	1	1	2.45
		GS15	3	1	4	1	2	1	3	3	3	4	4	1	1	2.45
		GS16	3	1	4	1	2	1	3	2	3	4	4	1	1	2.3
		GS17	1	1	4	1	2	1	3	3	4	4	4	1	1	2.35
		GS18	3	1	4	1	2	1	4	4	2	4	4	1	1	2.55
		GS19	2	1	4	1	2	1	4	3	2	4	4	1	1	2.3
		GS20	1	1	4	1	2	1	3	3	4	4	4	1	1	2.35
		GS21	3	1	4	1	2	1	3	3	3	4	4	1	1	2.45
		GS22	3	1	4	1	2	1	2	3	3	4	4	1	1	2.4
		GS23	1	1	4	1	2	1	2	2	3	4	4	1	1	2.05
		GS24	4	1	4	1	2	1	4	4	3	4	4	1	1	2.75
		GS25	2	1	4	1	2	1	3	4	2	4	4	1	1	2.4
		GS26	2	1	4	1	2	1	2	3	1	4	3	1	1	2

Table 4. Potential Education Use (PEU) matrix of the geosites in the region around the area of Option 4. The PEU values are also calculated at 1.2 and 4 points and represent the location's increasing values. The weight values for the total PEU calculation are given on the left side of the table.

PEU	Weight	Geosites	Vulnerability	Accessibility	Use Limitations	Safety	Logistics	Density Population	Association with Other Values	Scenery	Uniqueness	Observation Conditions	Didactic Potential	Geological Potential	Total Weighted
Vulnerability	10	GS1	4	1	4	1	2	1	4	2	2	4	2	3	2.45
Accessibility	10	GS2	4	1	4	1	2	1	4	2	2	4	2	3	2.45
Use limitations	5	GS3	3	1	4	1	2	1	4	3	4	4	2	1	2.3
Safety	10	GS4	4	1	4	1	2	1	3	4	4	4	2	3	2.6
Logistics	5	GS5	2	1	4	1	2	1	2	1	3	4	2	1	1.95
Density population	5	GS6	1	1	4	1	2	1	4	2	3	2	2	4	2.1
Other values	5	GS7	4	1	4	1	2	1	4	4	2	4	2	3	2.55
Scenery	5	GS8	3	1	4	1	2	1	2	3	3	4	2	1	2.15
Uniqueness	5	GS9	1	1	4	1	2	1	2	1	1	2	2	1	1.55
Observation conditions	10	GS10	3	1	4	1	2	1	2	3	2	4	2	2	2.2
Didactic potential	20	GS11	2	1	4	1	2	1	2	2	4	4	2	1	2.05
Geological potential	10	GS12	1	1	4	1	2	1	4	4	3	4	2	4	2.4
Total	100	GS13	3	1	4	1	2	1	4	3	1	4	2	2	2.25
		GS14	3	1	4	1	2	1	3	3	3	4	2	1	2.2
		GS15	3	1	4	1	2	1	3	3	3	4	2	2	2.3

Table 4. *Cont.*

GS16	3	1	4	1	2	1	3	2	3	4	2	2	2.25
GS17	1	1	4	1	2	1	3	3	4	4	2	2	2.15
GS18	3	1	4	1	2	1	4	4	2	4	2	3	2.45
GS19	2	1	4	1	2	1	4	3	2	4	2	3	2.3
GS20	1	1	4	1	2	1	3	3	4	4	2	2	2.15
GS21	3	1	4	1	2	1	3	3	3	4	2	1	2.2
GS22	3	1	4	1	2	1	2	3	3	4	2	2	2.25
GS23	1	1	4	1	2	1	2	2	3	4	2	1	1.9
GS24	4	1	4	1	2	1	4	4	3	4	2	4	2.7
GS25	2	1	4	1	2	1	3	4	2	4	2	2	2.2
GS26	2	1	4	1	2	1	2	3	1	4	2	2	2.05

Table 5. Degradation risk (DR) estimates a comparative matrix of the identified geosites in the region around the area of Option 4. The DR values are also calculated at 1, 2, and 4 points represent the location of increasing values. The weight values for the total PTU calculation are given on the left side of the table.

Degradation Risk	Weight	Geosites	Deterioration of Geological Elements	Proximity to Areas/Activities with Potential to Cause Degradation	Legal Protection	Accessibility	Density of Population	Total Weighted
Deterioration of geological elements	35	GS1	1	2	4	2	1	1.95
Proximity to areas/activities with potential to cause degradation	20	GS2	2	3	4	2	1	2.5
Legal protection	20	GS3	3	3	4	1	1	2.7
Accessibility	15	GS4	1	1	4	1	1	1.6
Density of population	10	GS5	2	2	4	2	1	2.3
Total	100	GS6	3	4	4	2	1	3.05
		GS7	1	1	4	1	1	1.6
		GS8	1	1	4	1	1	1.6
		GS9	3	3	4	2	1	2.85
		GS10	2	2	4	1	1	2.15
		GS11	2	2	4	1	1	2.15
		GS12	2	2	4	1	1	2.15
		GS13	2	2	4	1	1	2.15
		GS14	2	2	4	1	1	2.15
		GS15	2	2	4	1	1	2.15
		GS16	2	2	4	1	1	2.15
		GS17	4	2	4	1	1	2.85
		GS18	1	1	4	1	1	1.6
		GS19	1	1	4	1	1	1.6
		GS20	4	2	4	1	1	2.85
		GS21	2	2	4	1	1	2.15
		GS22	2	2	4	1	1	2.15
		GS23	4	2	4	1	1	2.85
		GS24	1	1	4	1	1	1.6
		GS25	1	1	4	1	1	1.6
		GS26	1	1	4	1	1	1.6

The Potential Education Use (PEU) (Table 4) assessment of the 26 geosites found that about half have strong potential. However, Brilha's method tends to favor sites near high visitation areas or with easy access, giving higher scores to those likely to attract many visitors. As a result, remote but geologically significant sites like Harrat Lunayyir are undervalued, despite their scientific importance.

Degradation risk (DR) assessments of the 26 geosites indicate a high likelihood of rapid deterioration, primarily due to insufficient legal protection and the area's vulnerability to human activities. Implementing formal protections and conducting science-based impact evaluations could significantly reduce this risk.

4. Discussion

The study region is a relatively remote, low population density area with an extensive dirt road network and tracks. The area is pristine, and its volcanic landscape can be considered a region where the basic characteristics of a typical basaltic monogenetic volcanic field geological features are well exposed, well preserved, and within a small area, representing all the known volcanic hazard types and their geological record. The arid conditions, while generating thick surficial deposits, especially along the major wadi network, have preserved the volcanic landforms exceptionally well, allowing for be able to see fine details of the scoria and spatter cone architectures and their extensive transitional pahoehoe lava flow fields. In global comparison, such intact volcanic regions are rare, and comparable places probably exist in the SW USA, NW Mexico, and some places in the arid regions in NE Africa. The advantage, however, in the case of Harrat Lunayyir, is that it is still accessible relatively easily, and the current tourism development initiatives can develop the region further to be a global reference point for continental monogenetic volcanic fields dominated by magmatic explosive and effusive processes. The estimated geoheritage values in combination with the geodiversity hot spots show that the key geosites are among those areas where the youngest volcanism occurred, leaving behind still intact volcanic landforms. For a regional comparison, while the volcanic fields' geoheritage has been documented in various studies in the last decade [36,37], relatively rare are those studies that qualitatively estimated a volcanic region's geoheritage values, especially their significance from a geotourism perspective [67]. In narrative description, it provides a good overview of the geoheritage and geodiversity of western Arabia, and, within that, Harrat Lunayyir is among the most compact regions (e.g., in the smallest areas, the greatest diversity of valley-confined lava flows, and typical magmatic explosive eruption-generated volcanic landforms preserved) [37]. In comparative perspective, there is a geosite, the Al Wahbah maar crater, that has been recently listed (2024) in the Second 100 International Union of Geosciences Geological Heritage list [https://iugs-geoheritage.org/geoheritage_sites/the-pleistocene-al-wahbah-dry-maar-crater/—accessed on 28 July 2025]; this geosite is where a Geosite Assessment was performed in 2012–2013 [67] and provides a good comparative site to see how the Option 4 area with its Target Volcano could perform against Al Wahbah maar. The calculations tabulated in Table 6 provide estimated values for the Option 4 area at Harrat Lunayyir. The data extracted from the 2012–2013 research from Al Wahbah represents relatively old data [67] that slightly changed as the Al Wahbah maar crater was listed in the Second 100 IUGS Geological Heritage Site list, and some tourism development increased the additional values of the region slightly. Still, the comparative analysis showed that while the current underdevelopment in tourism at Harrat Lunayyir is reducing the location's touristic value, its pristine nature as well as its young and still-active conditions, due to frequent volcano-seismic activity, compensate for the estimated values, indicating that a well-designed geotourism and geoconservation program would skyrocket Harrat Lunayyir to be a premier, globally significant location for geohazard resilience utilizing the region's volcanic geoheritage.

Table 6. Comparative table to demonstrate the study area geoheritage values in comparison to another geosite, now listed in the Second 100 IUGS Global Geological Heritage site list, Al Wahbah maar crater. The two sites were compared in their scientific and education values (VSE), scenic/aesthetic values (VSA), and protection (P). Functional and touristic values were also compared. The comparison showed that the study area stands strong for its global significance on its volcano science and untouched landscape beauty, but the area's touristic development is minimal.

Scientific, Education Values (VSE)	Al Wahbah	Narrative	Target Volcano + Qm5/6 Lava	Narrative
Rarity	0.75	one of the largest maar in Arabia.	0.75	one of the best-preserved young scoria cones with ash plain and complex lava flow field.
Representativeness	1	probably the most spectacular well-exposed maar crater.	1	perfect representation of a monogenetic explosive-effusive volcanic system with all known features well exposed.
Knowledge of geoscientific issues	1	international papers mention it.	0.75	the site is not but the region is mentioned internationally.
Level of interpretation	1	perfect site to understand maar-diatreme volcanoes.	1	perfect site to demonstrate complex eruption behavior of monogenetic volcanoes with unique lava flow fields.
Scenic/Aesthetic values (VSA)				
Viewpoints	1	view into crater from any point from rim, good panoramic view across plains.	1	perfect view of cones, complex lava fields, and the valley volcano has erupted.
Surface	1	area is about 10 km ² .	1	area is about 15 km ² .
Surrounding landscape and nature	0.75	view is attractive but not special from surrounding.	1	the young volcanic landscape characteristically distinct especially with the extensive ash plains.
Environmental fitting of sites	1	perfect representation of the location.	1	perfect representation of the location.
Protection (VPr)				
Current condition	0.75	some local rubbish dumped at main viewpoints.	1	pristine.
Protection level	0.5	some regional legal protection.	0	none.
Vulnerability	0.75	visitor driven damage is probable if visitation increases.	0.5	especially the ash plains are very vulnerable to natural and human-induced impact.
Suitable number of visitors	1	more than 50.	0.5	probably small group of 10–20 in one round.
Total (VSE + VSA + VPr)	10.5		9.5	
Functional values (VFn)				
Accessibility	0.75	by car.	0.25	by foot, special equipment.
Additional natural values	1	ecosystem in crater.	1	complex ecosystem.
Additional anthropogenic values	0.25	plantations in crater wall.	1	rich geoarchaeology in the region.
Vicinity to emission centers	0.25		0	
Vicinity to important road network	0.75		0.75	
Additional functional values	0.75		0.5	
Touristic values (VTr)				

Table 6. Cont.

Scientific, Education Values (VSE)	Al Wahbah	Narrative	Target Volcano + Qm5/6 Lava	Narrative
Promotion	1	One of the IUGS F100 site.	0	none currently.
Annual number of organized visits	0.75		0.25	
Vicinity to visitor's center	1	on site.	0.25	
Interpretative panels	0.25	low quality.	0	none currently.
Annual number of visitors	0.25	less than 5000.	0	few dozen.
Tourism infrastructure	0.75		0	
Tour guide service	0.25		0	
Hostelry service	0.25		0.25	
Restaurant service	0		0	
Total (VFn + VTr)	8.25		4.25	

The volcano-seismic activity of the region and the identified volcanic hazard scenarios provided important information to investors; namely, that any development in the region faces a significant volcano-seismic hazard that is also highly unpredictable. While the hazard estimates indicate relatively low intensity hazard types, their potential destructive power, or hazard appetite, could be considerably large, including destruction of the built environment by lava flows that are difficult to control if the eruption initiates [70,71]. This finding, and the exceptional geoheritage values of the well-preserved geo-features representing specific, key volcanic hazard elements, suggest that geoconservation and geohazard education could play a key role in future geotourism development in the region. This is perfectly justified by the pristine natural volcanic environment that is a globally rare feature, especially its well-defined geographical extent and the relatively slow recurrence rate of volcanism expected in the region (e.g., in the Harrat Lunayyir no active volcanism tourism operation needs to be dealt with, while the preserved landscape mimics a landscape that provides an impression that it was created very recently). In hazard and risk estimates, for medium-to-long term tourism development, it is more beneficial to invest in geoconservation and preservation of the pristine volcanic landscape to use it for scientific research as well as geoeducation through geotourism managed through daily guided visits and low-investment site development, geotrail design, and geoguide trainings to reduce the potential risk of loss of built facilities in the case of volcano-seismic unrest. This approach would likely be accompanied by a strong link between hazard specialists and responsible monitoring entities to maximize the region's volcanic geoheritage use for geohazard communication to the local communities, as well as for visitors. This research originated from a comprehensive geohazard assessment of the region, which revealed significant volcano-seismic hazards [70]. Recognizing the volcanic geoheritage could benefit geohazard education, communication, community initiatives, citizen science, and collaborative hazard mitigation between the Saudi Geological Survey, as a main volcano-seismic monitoring agency, and future tourism developers. Ideally, a co-developed hazard management system between tourism operators, investors, and the Saudi Geological Survey would be an ideal operational scenario to train tourism operators on what to do and how to act upon a volcano-seismic crisis that might strike in the future.

Our research also has strong limitations. Each site included in the GCR in the UK was selected using a combination of published and unpublished records, input from subject specialists, direct site assessment, and review of relevant materials from museums or other collections. Although comprehensive adoption of the Wimbledon method for geosite inventory was not feasible due to limited published material at the required scale, the selection process relied on evaluating the geological significance of features from a broad geological perspective. For example, a scoria cone was assessed by comparison with examples documented in the research literature. This allowed for the determination of the scientific significance of regional geosites and their research potential. The approach proved effective for identifying and justifying sites from a geohazard standpoint, highlighting their role in volcanic hazard education and community resilience.

Countries with strong research backgrounds can engage a wide range of experts in geosite recognition, though expertise may still vary across topics. In well-studied fields, the process shifts to interpreting inputs from specialists and comparing sites based on features like stratigraphy, sediments, macrofossils, and dating methods. Justifying each site requires distinguishing typical from unique characteristics. This study represents an initial attempt to identify priority geosites, mainly for volcanic hazards, highlighting the need for broader, more uniform research across the region. In areas lacking geological studies, rapid assessment of geodiversity hotspots using basic data can guide future

efforts. Focusing on specific geological processes can help define relevant segments for geoeducation, conservation, and visitation programs.

5. Conclusions

This report identifies the principal rock types, structural features, and geoheritage values present in the study area. The findings establish a solid foundation for developing a comprehensive and informative geological map of the region, with a particular focus on the Option 4 area, which will be addressed in detail in the subsequent report.

Volcanic and seismic hazard evaluations indicate that any future development will require significant research to better understand the region's geohazards. Collaborative efforts among end-users, investors, and scientists are recommended to develop effective mitigation strategies, with their results being geotourism development with an aim to offer geoeducation toward establishing a geohazard resilient community. Research suggests that further development should consider the geoheritage and geodiversity values of the area, which may offer a foundation for evidence-based geoheritage initiatives. These could include geoconservation, volcanic hazard education, and geoeducation through limited and controlled visitation, alongside the possible establishment of a geoheritage reserve to maintain the region's current state. The site contains notable geological features that could be relevant for volcanic hazard resilience programs for both local communities and visitors. This article presented an estimate of the region's geodiversity and provides systematic data to support the significance of its geoheritage, potentially contributing to applications for designations such as local, regional, or UNESCO Global Geopark status.

The primary conclusion of this work is that the Option 4 area exhibits exceptional geological and geomorphological diversity, providing strong justification for potential geotourism development. The region has also been recognized as a geodiversity hotspot, with 26 distinct geosites nominated. These geosites were evaluated using globally recognized methodologies, and all met the criteria necessary for consideration in future geotourism and geoeducation initiatives. However, it should be noted that nearly half of these geosites are in highly fragile environments, necessitating robust conservation measures to preserve their integrity and minimize the risk of degradation. To utilize the region, volcanic geoheritage for geohazard education geotrail development can offer sustainable landscape management, highlighting the area's detailed volcanological features that can enhance geoeducational opportunities.

This research has limitations, highlighting the need for further study. It focused on a specifically defined region planned for tourism, with geosite selections based on basic criteria. Future work should use more uniform, evidence-based site selection across the volcanic field to better understand its geoheritage structure compared to existing geological values. Objective assessment may require expert involvement. Testing the representativeness of geological elements for geohazard parameters is also recommended, using participatory methods with local communities and tourism investors for hazard management and geotourism development. No systematic comparison was made with similar areas elsewhere, but ongoing research aims to enhance rural nature-based tourism in the region.

However, tourism and accessibility remain underdeveloped. As a result, Option 4 presents the most suitable site for geotourism and geoeducation development; nevertheless, improvements in local tourism and infrastructure could enhance geosite value while simultaneously increasing degradation risk. Consequently, it is essential to balance these competing trends through strategic planning.

Author Contributions: Conceptualization, K.N. and V.Z.; methodology, K.N. and V.Z.; software, A.S. and V.Z.; validation, K.N., M.T., M.A., V.S., F.M., T.H., T.S., K.A. and K.Y.; formal analysis, K.N.

and V.Z.; investigation, K.N.; resources, K.N., A.S., T.S. and K.Y.; data curation, K.N., A.S. and V.Z.; writing—original draft preparation, K.N.; writing—review and editing, A.S., M.T., M.A., V.S., F.M., K.A., T.H., T.S. and K.Y.; visualization, K.N., A.S. and V.Z.; supervision, K.N.; project administration, A.S.; funding acquisition, K.N., A.S., T.S. and K.Y. All authors have read and agreed to the published version of the manuscript.

Funding: This research was funded by Red Sea Global—Saudi Geological Survey Contract: C00-O00D14-Black Desert-Volcano Hazard Assessment Contract (Saudi Geological Survey).

Data Availability Statement: All data used in this research is used in the manuscript presented here.

Acknowledgments: We are acknowledging the support given to conduct this research by the National Program of Earthquakes and Volcanoes of the Saudi Geological Survey. The authors are also thankful for the reviewers' constructive comments and the journal's invitation to contribute to this volume.

Conflicts of Interest: The authors declare no conflicts of interest.

References

1. Brilha, J.; Reynard, E. Geoheritage and geoconservation: The challenges. In *Geoheritage: Assessment, Protection, and Management*, 1st ed.; Elsevier: Amsterdam, The Netherlands, 2018; pp. 433–438. ISBN 978-0-12-809531-7.
2. Reynard, E.; Brilha, J. Geoheritage: A multidisciplinary and applied research topic. In *Geoheritage: Assessment, Protection, and Management*, 1st ed.; Elsevier: Amsterdam, The Netherlands, 2018; pp. 3–9. ISBN 978-0-12-809531-7.
3. Bentivenga, M.; Cavalcante, F.; Mastronuzzi, G.; Palladino, G.; Prosser, G. Geoheritage: The Foundation for Sustainable Geotourism. *Geoheritage* **2019**, *11*, 1367–1369. [CrossRef]
4. Bentivenga, M.; Geremia, F. VII international symposium progeo on the conservation of the geological heritage 'Geoheritage: Protecting and sharing', Bari (Apulia, Italy), 24th to 28th September 2012. *Geoheritage* **2015**, *7*, 1–3. [CrossRef]
5. Pescatore, E.; Bentivenga, M.; Giano, S.I. Geoheritage Management in Areas with Multicultural Interest Contexts. *Sustainability* **2022**, *14*, 5911. [CrossRef]
6. Pescatore, E.; Bentivenga, M.; Giano, S.I. Geoheritage and Geoconservation: Some Remarks and Considerations. *Sustainability* **2023**, *15*, 5823. [CrossRef]
7. Bentivenga, M.; Pescatore, E.; Piccarreta, M.; Gizzi, F.T.; Masini, N.; Giano, S.I. Geoheritage and Geoconservation, from Theory to Practice: The Ghost Town of Craco (Matera District, Basilicata Region, Southern Italy). *Sustainability* **2024**, *16*, 2761. [CrossRef]
8. Geremia, F.; Bentivenga, M.; Palladino, G. Environmental geology applied to geoconservation in the interaction between geosites and linear infrastructures in South-Eastern Italy. *Geoheritage* **2015**, *7*, 33–46. [CrossRef]
9. Giano, S.I.; Pescatore, E.; Biscione, M.; Masini, N.; Bentivenga, M. Geo- and Archaeo-heritage in the Mount Vulture Area: List, Data Management, Communication, and Dissemination. A Preliminary note. *Geoheritage* **2022**, *14*, 10. [CrossRef]
10. Wimbledon, W.A. The development of a methodology for the selection of British geological sites for conservation: Part 1. *Mod. Geol.* **1995**, *20*, 159–202.
11. Brocx, M.; Semeniuk, V. Geoheritage and geoconservation-history, definition, scope and scale. *J. R. Soc. West. Aust.* **2007**, *90*, 53–87.
12. Dowling, R.K.; Newsome, D. *Geotourism*; Routledge: London, UK, 2005; pp. 1–260. [CrossRef]
13. Newsome, D.; Moore, S.A.; Dowling, R.K. *Natural Area Tourism: Ecology, Impacts and Management*; Channel View Publications: Bristol, UK, 2013; pp. 1–504. ISBN 978-1-84541-381-1.
14. Dowling, R. Geotourism's contribution to sustainable tourism. In *The Practice of Sustainable Tourism: Resolving the Paradox*; Routledge: London, UK, 2015; pp. 207–227. ISBN 9781315796154.
15. Dowling, R.; Newsome, D. Geotourism: Definition, characteristics and international perspectives. In *Handbook of Geotourism*; Edward Elgar Publishing Ltd.: Cheltenham, UK, 2018; pp. 1–22. ISBN 978 1 78536 885 1.
16. Wang, J.; Zouros, N. Educational Activities in Fangshan UNESCO Global Geopark and Lesvos Island UNESCO Global Geopark. *Geoheritage* **2021**, *13*, 51. [CrossRef]
17. Zafeiropoulos, G.; Drinia, H.; Antonarakou, A.; Zouros, N. From geoheritage to geoeducation, geoethics and geotourism: A critical evaluation of the Greek region. *Geosciences* **2021**, *11*, 381. [CrossRef]
18. Golfinopoulos, V.; Papadopoulou, P.; Koumoutsou, E.; Zouros, N.; Fassoulas, C.; Zelilidis, A.; Iliopoulos, G. Quantitative Assessment of the Geosites of Chelmos-Vouraikos UNESCO Global Geopark (Greece). *Geosciences* **2022**, *12*, 63. [CrossRef]
19. Ceballos-Lascuráin, H. *Tourism, Ecotourism, and Protected Areas: The State of Nature-Based Tourism Around the World and Guidelines for Its Development*; IUCN: Gland, Switzerland, 1996; 301p, ISBN 978-2-8317-0124-0. Available online: <https://portals.iucn.org/library/node/7006> (accessed on 2 September 2025).

20. Valjarević, A.; Vukoičić, D.; Valjarević, D. Evaluation of the tourist potential and natural attractivity of the Lukovska Spa. *Tour. Manag. Perspect.* **2017**, *22*, 7–16. [CrossRef]
21. Reynard, E.; Giusti, C. Chapter 8—The Landscape and the Cultural Value of Geoheritage. In *Geoheritage*; Reynard, E., Brilha, J., Eds.; Elsevier: Amsterdam, The Netherlands, 2018; pp. 147–166.
22. Martí-Molist, J.; Dorado-García, O.; López-Saavedra, M. The Volcanic Geoheritage of El Teide National Park (Tenerife, Canary Islands, Spain). *Geoheritage* **2022**, *14*, 65. [CrossRef]
23. Dóniz-Páez, J.; Alonso, C.Q. Urban geotourism routes in Icod de los Vinos (Tenerife, Canary Islands, Spain): A proposal. *Cuad. Geogr.* **2016**, *55*, 320–343.
24. Dóniz-Páez, J.; Beltrán-Yanes, E.; Becerra-Ramírez, R.; Pérez, N.M.; Hernández, P.A.; Hernández, W. Diversity of volcanic geoheritage in the Canary Islands, Spain. *Geosciences* **2020**, *10*, 390. [CrossRef]
25. Hernández, W.; Dóniz-Páez, J.; Pérez, N.M. Urban Geotourism in La Palma, Canary Islands, Spain. *Land* **2022**, *11*, 1337. [CrossRef]
26. Dóniz-Páez, J.; Becerra-Ramírez, R.; Németh, K.; Gosálvez, R.U.; Lahoz, E.E. Geomorfositos de interés geoturístico del volcán monogenético Tajogaite, erupción de 2021 (La Palma, Islas Canarias, España). *Geofis. Int.* **2024**, *63*, 731–748. [CrossRef]
27. Ramos, W.H.; Dóniz-Páez, J.; García-Hernández, R.; Pérez, N.M. Evaluation of Sites of Geotouristic Interest on Active Volcanic Island La Palma, Spain for Potential Volcanic Tourism. *Geoheritage* **2024**, *16*, 102. [CrossRef]
28. Guevara, D.; Becerra-Ramírez, R.; Dóniz-Páez, J.; Escobar, E. Proposal of an Urban Geotourism Itinerary in the UNESCO Global Geopark Volcanes de Calatrava, Ciudad Real (Castilla-La Mancha, Spain): “Volcanoes and Petra Bona (Piedrabuena)”. *Land* **2025**, *14*, 1363. [CrossRef]
29. Németh, K.; Casadevall, T.; Moufti, M.R.; Martí, J. Volcanic Geoheritage. *Geoheritage* **2017**, *9*, 251–254. [CrossRef]
30. Németh, K.; Wu, J.; Sun, C.; Liu, J. Update on the Volcanic Geoheritage Values of the Pliocene to Quaternary Arxan–Chaihe Volcanic Field, Inner Mongolia, China. *Geoheritage* **2017**, *9*, 279–297. [CrossRef]
31. Aleksova, B.; Vasiljević, D.; Németh, K.; Milevski, I. Palaeovolcanic Geoheritage from Volcano Geology Perspective within Earth’s Geosystems: Geoeducation of the Potential Geopark Kratovo–Zletovo (North Macedonia). *Geoheritage* **2024**, *16*, 54. [CrossRef]
32. Casadevall, T.J.; Tormey, D.; Van Sistine, D. Protecting our global volcanic estate: Review of international conservation efforts. *Int. J. Geoherit. Parks* **2019**, *7*, 182–191. [CrossRef]
33. Keever, P.M.; Narbonne, G.M. *Geological World Heritage: A Revised Global Framework for the Application of Criterion (VIII) of the World Heritage Convention*; IUCN: Gland, Switzerland, 2021; ISBN 978-2-8317-2141-5. [CrossRef]
34. Migoñ, P. Chapter 13—Geoheritage and World Heritage Sites. In *Geoheritage*; Reynard, E., Brilha, J., Eds.; Elsevier: Amsterdam, The Netherlands, 2018; pp. 237–249.
35. Hilario, A.; Asrat, A.; de Vries, B.v.W.; Mogk, D.; Lozano, G.; Zhang, J.; Brilha, J.; Vegas, J.; Lemon, K.; Carcavilla, L. *The First 100 IUGS Geological Heritage Sites*; International Union of Geological Sciences (IUGS): Beijing, China, 2022.
36. Moufti, M.R.; Németh, K. *Geoheritage of Volcanic Harrats in Saudi Arabia*; Springer: Berlin/Heidelberg, Germany, 2016; pp. 1–194.
37. Németh, K.; Moufti, M.R.H. Systematic Overview of the Geoheritage and Geodiversity of Monogenetic Volcanic Fields of Saudi Arabia. In *Geoheritage and Geodiversity of Cenozoic Volcanic Fields in Saudi Arabia: Challenges of Geoconservation and Geotourism in a Changing Environment*; Németh, K., Moufti, M.R.H., Eds.; Springer Nature: Cham, Switzerland, 2024; pp. 33–124.
38. Moufti, M.R.; Németh, K.; El-Masry, N.; Qaddah, A. Volcanic Geotopes and Their Geosites Preserved in an Arid Climate Related to Landscape and Climate Changes Since the Neogene in Northern Saudi Arabia: Harrat Hutaymah (Hai’il Region). *Geoheritage* **2015**, *7*, 103–118. [CrossRef]
39. Duncan, R.A.; Al-Amri, A.M. Timing and composition of volcanic activity at Harrat Lunayyir, western Saudi Arabia. *J. Volcanol. Geotherm. Res.* **2013**, *260*, 103–116. [CrossRef]
40. Pallister, J.S.; McCausland, W.A.; Jónsson, S.; Lu, Z.; Zahran, H.M.; El Hadidy, S.; Aburukbah, A.; Stewart, I.C.F.; Lundgren, P.R.; White, R.A.; et al. Broad accommodation of rift-related extension recorded by dyke intrusion in Saudi Arabia. *Nat. Geosci.* **2010**, *3*, 705–712. [CrossRef]
41. Saibi, H.; Mogren, S.; Mukhopadhyay, M.; Ibrahim, E. Subsurface imaging of the Harrat Lunayyir 2007–2009 earthquake swarm zone, western Saudi Arabia, using potential field methods. *J. Asian Earth Sci.* **2019**, *169*, 79–92. [CrossRef]
42. Xu, W.; Jónsson, S.; Corbi, F.; Rivalta, E. Graben formation and dike arrest during the 2009 Harrat Lunayyir dike intrusion in Saudi Arabia: Insights from InSAR, stress calculations and analog experiments. *J. Geophys. Res. Solid Earth* **2016**, *121*, 2837–2851. [CrossRef]
43. Zahran, H.M.; El-Hady, S.M. Seismic hazard assessment for Harrat Lunayyir—A lava field in western Saudi Arabia. *Soil Dyn. Earthq. Eng.* **2017**, *100*, 428–444. [CrossRef]
44. Zobin, V.M.; Al-Amri, A.M.; Fnaiss, M. Seismicity associated with active, new-born, and re-awakening basaltic volcanoes: Case review and the possible scenarios for the Harraat volcanic provinces, Saudi Arabia. *Arab. J. Geosci.* **2013**, *6*, 529–541. [CrossRef]
45. Singtuen, V.; Srisaphon, S. Exploring the Distribution and Occurrence of Cenozoic Volcanic Geoheritages in the Khorat Plateau, Thailand. *Quaest. Geogr.* **2025**. *in press*. Available online: <https://sciendo.com/article/10.14746/quageo-2025-0031> (accessed on 2 September 2025).

46. Mülâyim, O.; Köroğlu, F.; Alkaç, O. Volcanic Geoheritage and Geotourism Values of the Siverek Columnar Basalts, Şanlıurfa (SE Türkiye). *Geoheritage* **2025**, *17*, 103. [\[CrossRef\]](#)
47. Arias, C.; de Vries, B.V.W.; Aguilar, R.; Mariño, J.; Cueva, K.; Manrique, N.; Zavala, B.; Ancalle, A. Volcanic geoheritage in Arequipa, Southern Peru: Assessment of pilot geosites for geohazard resilience. *Int. J. Geohérit. Parks* **2025**, *13*, 44–67. [\[CrossRef\]](#)
48. Migoń, P.; Pijet-Migoń, E. Geoconservation History of a Basalt Quarry—The Case of Mt. Wilkołak, Land of Extinct Volcanoes Geopark, SW Poland. *Geoheritage* **2024**, *16*, 65. [\[CrossRef\]](#)
49. Jeon, Y.; Ki, J.; Southcott, D. Korean geoheritage: The volcanic landforms of the Jeju Island UNESCO Global Geopark. *Episodes* **2024**, *47*, 295–310. [\[CrossRef\]](#) [\[PubMed\]](#)
50. Sheth, H. The Volcanic Geoheritage of the Ajanta and Ellora Caves, Central Deccan Traps, India. *Geoheritage* **2023**, *15*, 39. [\[CrossRef\]](#)
51. Alfama, V.; Henriques, M.H.; Barros, A. The Challenging Nature of Volcanic Heritage: The Fogo Island (Cabo Verde, W Africa). *Geoheritage* **2024**, *16*, 34. [\[CrossRef\]](#)
52. Quesada-Román, A.; Zangmo, G.T.; Pérez-Umaña, D. Geomorphosite Comparative Analysis in Costa Rica and Cameroon Volcanoes. *Geoheritage* **2020**, *12*, 90. [\[CrossRef\]](#)
53. Mehdiipour Ghazi, J.; Audra, P. Travertine Park in Azarshahr (NW Iran): An Opportunity for Geoheritage Conservation and Diminishing Geohazards Risk. *Geoheritage* **2022**, *14*, 99. [\[CrossRef\]](#)
54. Novković, I.; Dragičević, S.; Djurović, M. Geohazard and Geoheritage. In *World Regional Geography Book Series*; Springer: Cham, Switzerland, 2022; pp. 119–131. ISBN 978-3-030-74700-8.
55. Kubalíková, L.; Irapta, P.N.; Pál, M.; Zwolinski, Z.; Coratza, P.; Vries, B.W. Visages of geodiversity and geoheritage: A multidisciplinary approach to valuing, conserving and managing abiotic nature. *Geol. Soc. Spec. Publ.* **2023**, *530*, 1–12. [\[CrossRef\]](#)
56. Hoyland, R.O.; McHenry, M.T. Modelling Relative Fire Sensitivity for Geodiversity Elements. *Fire* **2025**, *8*, 101. [\[CrossRef\]](#)
57. Knight, J.; Grab, S.W. Vulnerability of geoheritage sites in South Africa to climate change: Examples from the Eastern Cape Province. *Geomorphology* **2024**, *457*, 109246. [\[CrossRef\]](#)
58. Agastya, I.B.O.; Diwyastira, P.D.; Hespianito, S.; Ariana, D. Geological Disaster Hazard Mapping Based on Geoheritage: A Case Study of the Batur UNESCO Global Geopark. *IOP Conf. Ser. Earth Environ. Sci.* **2024**, *1424*, 012027. [\[CrossRef\]](#)
59. Vidal, R.R.; Tassara, A. Geo-Circuit for Interpretation of the Geological Evolution in the Nevados de Chillán Volcanic Complex, Chile. *Geoheritage* **2023**, *15*, 63. [\[CrossRef\]](#)
60. Németh, B.; Németh, K. Spatial decision-making support for geoheritage conservation in the urban and indigenous environment of the Auckland Volcanic Field, New Zealand. *Geol. Soc. Spec. Publ.* **2023**, *530*, 235–256. [\[CrossRef\]](#)
61. Avagyan, A.; Sahakyan, L.; Meliksetyan, K.; Hovhannisyan, A.; Arakelyan, D.; Galoyan, G.; Melik-Adamyan, H.; Grigoryan, T.; Sahakyan, K.; Grigoryan, E.; et al. The Potential for a Geohazard-Related Geopark in Armenia. *Geoheritage* **2023**, *15*, 133. [\[CrossRef\]](#)
62. Guilbaud, M.N.; Ortega-Larrocea, M.P.; Cram, S.; van Wyk de Vries, B. Xitle Volcano Geoheritage, Mexico City: Raising Awareness of Natural Hazards and Environmental Sustainability in Active Volcanic Areas. *Geoheritage* **2021**, *13*, 6. [\[CrossRef\]](#)
63. Ertekin, C.; Ekinci, Y.L.; Büyüksaraç, A.; Ekinci, R. Geoheritage in a Mythical and Volcanic Terrain: An Inventory and Assessment Study for Geopark and Geotourism, Nemrut Volcano (Bitlis, Eastern Turkey). *Geoheritage* **2021**, *13*, 73. [\[CrossRef\]](#)
64. Vereb, V.; van Wyk de Vries, B.; Hagos, M.; Karátson, D. Geoheritage and Resilience of Dallol and the Northern Danakil Depression in Ethiopia. *Geoheritage* **2020**, *12*, 82. [\[CrossRef\]](#)
65. Scarlett, J.P.; Riede, F. The Dark Geocultural Heritage of Volcanoes: Combining Cultural and Geoheritage Perspectives for Mutual Benefit. *Geoheritage* **2019**, *11*, 1705–1721. [\[CrossRef\]](#)
66. Fepuleai, A.; Németh, K. Volcanic Geoheritage of Landslides and Rockfalls on a Tropical Ocean Island (Western Samoa, SW Pacific). *Geoheritage* **2019**, *11*, 577–596. [\[CrossRef\]](#)
67. Moufti, M.R.; Németh, K.; El-Masry, N.; Qaddah, A. Geoheritage values of one of the largest maar craters in the Arabian Peninsula: The Al Wahbah Crater and other volcanoes (Harrat Kishb, Saudi Arabia). *Cent. Eur. J. Geosci.* **2013**, *5*, 254–271. [\[CrossRef\]](#)
68. Németh, K.; Kereszturi, G. Monogenetic volcanism: Personal views and discussion. *Int. J. Earth Sci.* **2015**, *104*, 2131–2146. [\[CrossRef\]](#)
69. Muzambiq, S.; Walid, H.; Ganie, T.H.; Hermawan, H. The Importance of Public Education and Interpretation in the Conservation of Toba Caldera Geoheritage. *Geoheritage* **2021**, *13*, 3. [\[CrossRef\]](#)
70. Németh, K.; Toni, M.; Sokolov, V.; Sowaigh, A.; Ashor, M.; Moqem, F. Eruption Scenarios of a Monogenetic Volcanic Field Formed within a Structurally Controlled Basement Terrain: Harrat Lunayyir, Saudi Arabia. In *A Comprehensive Study of Volcanic Phenomena*; Németh, K., Ed.; IntechOpen: Rijeka, Croatia, 2024.
71. Németh, K.; Sowaigh, A.; Toni, M.; Sokolov, V.; Moqem, F. Volcanic hazard assessment of northern Harrat Lunayyir, Kingdom of Saudi Arabia: Volume 5 of 5. In *Saudi Geological Survey Project Contract Report*; SGS-PCR-2024-2 (Volume 5 of 5); Saudi Geological Survey: Jeddah, Saudi Arabia, 2025; p. 68.
72. Johnson, P.R.; Kattan, F. Oblique sinistral transpression in the Arabian shield: The timing and kinematics of a Neoproterozoic suture zone. *Precamb. Res.* **2001**, *107*, 117–138. [\[CrossRef\]](#)

73. Johnson, P.R.; Stewart, I.C.F. Magnetically inferred basement structure in central Saudi Arabia. *Tectonophysics* **1995**, *245*, 37–52. [\[CrossRef\]](#)
74. Brilha, J. Geoheritage. In *Encyclopedia of Geology: Volume 1–6*, 2nd ed.; Elsevier: Amsterdam, The Netherlands, 2020; Volume 6, pp. 569–578.
75. Prosser, C.D.; Díaz-Martínez, E.; Larwood, J.G. Chapter 11—The Conservation of Geosites: Principles and Practice. In *Geoheritage: Assessment, Protection, and Management*, 1st ed.; Reynard, E., Brilha, J., Eds.; Elsevier: Amsterdam, The Netherlands, 2018; pp. 193–212. ISBN 978-0-12-809531-7.
76. Brilha, J. Geoheritage: Inventories and evaluation. In *Geoheritage: Assessment, Protection, and Management*, 1st ed.; Reynard, E., Brilha, J., Eds.; Elsevier: Amsterdam, The Netherlands, 2018; pp. 69–85. ISBN 978-0-12-809531-7.
77. Brilha, J. Chapter 18—Geoheritage and Geoparks. In *Geoheritage: Assessment, Protection, and Management*, 1st ed.; Reynard, E., Brilha, J., Eds.; Elsevier: Amsterdam, The Netherlands, 2018; pp. 323–335. ISBN 978-0-12-809531-7.
78. Gray, M. Other nature: Geodiversity and geosystem services. *Environ. Conserv.* **2011**, *38*, 271–274. [\[CrossRef\]](#)
79. Gray, M. Geodiversity: The origin and evolution of a paradigm. *Geol. Soc. Spec. Publ.* **2008**, *300*, 31–36. [\[CrossRef\]](#)
80. Brilha, J.; Gray, M.; Pereira, D.I.; Pereira, P. Geodiversity: An integrative review as a contribution to the sustainable management of the whole of nature. *Environ. Sci. Policy* **2018**, *86*, 19–28. [\[CrossRef\]](#)
81. Coratza, P.; Reynard, E.; Zwoliński, Z. Geodiversity and Geoheritage: Crossing Disciplines and Approaches. *Geoheritage* **2018**, *10*, 525–526. [\[CrossRef\]](#)
82. Crofts, R. Promoting geodiversity: Learning lessons from biodiversity. *Proc. Geol. Assoc.* **2014**, *125*, 263–266. [\[CrossRef\]](#)
83. Zakharovskiy, V.; Németh, K. Quantitative-qualitative method for quick assessment of geodiversity. *Land* **2021**, *10*, 946. [\[CrossRef\]](#)
84. Li, B.X.; Németh, K.; Zakharovskiy, V.; Palmer, J.; Palmer, A.; Proctor, J. Geodiversity estimate of the Arxan–Chaihe Volcanic Field extending across two geoparks in Inner Mongolia, NE China. *Geol. Soc. Spec. Publ.* **2023**, *530*, 107–125. [\[CrossRef\]](#)
85. Zakharovskiy, V.; Németh, K.; Gravis, I.; Twemlow, C. Geosite Recognition Based on Qualitative–Quantitative Assessment in the Light of Core Geological Features of a Mio-Pliocene Volcanic Arc Setting of the Coromandel Peninsula, New Zealand. *Geoheritage* **2024**, *16*, 19. [\[CrossRef\]](#)
86. Wimbledon, W.A.P. National site selection, a stop on the road to a European Geosite list. *Geol. Balc.* **1996**, *26*, 15–27.
87. Brilha, J. Inventory and Quantitative Assessment of Geosites and Geodiversity Sites: A Review. *Geoheritage* **2016**, *8*, 119–134. [\[CrossRef\]](#)
88. Sen, S.; Abouelresh, M.O.; Santra, A.; Al-Musabeh, A.H.; Al-Ismail, F.S. Geoheritage Assessment of the Geosites in Tuwaiq Mountain, Saudi Arabia: In the Perspective of Geoethics, Geotourism, and Geoconservation. *Geoheritage* **2024**, *16*, 2. [\[CrossRef\]](#)
89. Sen, S.; Abouelresh, M.O.; Joydas, T.V.; Almusabeh, A.; Al-Ismail, F.S.; Pulido, B. Geoheritage and Geotourism Potential of NEOM, Saudi Arabia: Linking Geoethics, Geoconservation, and Geotourism. *Geoheritage* **2024**, *16*, 27. [\[CrossRef\]](#)
90. Sen, S.; Almusabeh, A.; Abouelresh, M.O. Geoheritage and Geotourism Potential of Tuwaiq Mountain, Saudi Arabia. *Geoheritage* **2023**, *15*, 93. [\[CrossRef\]](#)
91. Al Mohaya, J.; Elassal, M. Assessment of Geosites and Geotouristic Sites for Mapping Geotourism: A Case Study of Al-Soudah, Asir Region, Saudi Arabia. *Geoheritage* **2023**, *15*, 7. [\[CrossRef\]](#)
92. Stern, R.J.; Johnson, P. Continental lithosphere of the Arabian Plate: A geologic, petrologic, and geophysical synthesis. *Earth-Sci. Rev.* **2010**, *101*, 29–67. [\[CrossRef\]](#)
93. Johnson, C.A. Phanerozoic plate reconstructions of the middle east: Insights into the context of arabian tectonics and sedimentation. In Proceedings of the Society of Petroleum Engineers-13th Abu Dhabi International Petroleum Exhibition and Conference, ADIPEC 2008, Abu Dhabi, United Arab Emirates, 3–6 November 2008; pp. 1242–1257.
94. Nehlig, P.; Antonin, G.; Asfirane, F. A review of the Pan-African evolution of the Arabian Shield. *Geoarabia* **2002**, *7*, 103–124. [\[CrossRef\]](#)
95. Stern, R.J.; Mukherjee, S.K.; Miller, N.R.; Ali, K.; Johnson, P.R. ~750 Ma banded iron formation from the Arabian-Nubian Shield—Implications for understanding neoproterozoic tectonics, volcanism, and climate change. *Precamb. Res.* **2013**, *239*, 79–94. [\[CrossRef\]](#)
96. Camp, V.E.; Roobol, M.J. Upwelling asthenosphere beneath Western Arabia and its regional implications. *J. Geophys. Res.-Solid Earth* **1992**, *97*, 15255–15271. [\[CrossRef\]](#)
97. Hassan Ahmed, A. Geology and Lithostratigraphy of the Arabian–Nubian Shield. In *Mineral Deposits and Occurrences in the Arabian–Nubian Shield*; Hassan Ahmed, A., Ed.; Springer International Publishing: Cham, Switzerland, 2022; pp. 1–67.
98. Stern, R.J. Arc assembly and continental collision in the Neoproterozoic East African Orogen: Implications for the consolidation of Gondwanaland. *Annu. Rev. Earth Planet. Sci.* **1994**, *22*, 319–351. [\[CrossRef\]](#)
99. Stein, M.; Goldstein, S.L. From plume head to continental lithosphere in the Arabian–Nubian shield. *Nature* **1996**, *382*, 773–778. [\[CrossRef\]](#)
100. Self, S.; Keszthelyi, L.; Thordarson, T. The importance of pāhoehoe. *Annu. Rev. Earth Planet. Sci.* **1998**, *26*, 81–110. [\[CrossRef\]](#)
101. Keszthelyi, L.P.; Pieri, D.C. Emplacement of the 75-km-long Carrizozo lava flow field, south-central New Mexico. *J. Volcanol. Geotherm. Res.* **1993**, *59*, 59–75. [\[CrossRef\]](#)

102. Self, S.; Thordarson, T.; Keszthelyi, L.; Walker, G.P.L.; Hon, K.; Murphy, M.T.; Long, P.; Finnemore, S. A new model for the emplacement of Columbia River basalts as large, inflated pahoehoe lava flow fields. *Geophys. Res. Lett.* **1996**, *23*, 2689–2692. [\[CrossRef\]](#)
103. Gregg, T.K.P.; Keszthelyi, L.P. The emplacement of pahoehoe toes: Field observations and comparison to laboratory simulations. *Bull. Volcanol.* **2004**, *66*, 381–391. [\[CrossRef\]](#)
104. Keszthelyi, L.; Denlinger, R. The initial cooling of pahoehoe flow lobes. *Bull. Volcanol.* **1996**, *58*, 5–18. [\[CrossRef\]](#)
105. Cashman, K.V.; Thornber, C.; Kauahikaua, J.P. Cooling and crystallization of lava in open channels, and the transition of Pāhoehoe Lava to ‘A‘ā. *Bull. Volcanol.* **1999**, *61*, 306–323. [\[CrossRef\]](#)
106. Rowland, S.K.; Walker, G.P.L. Toothpaste lava: Characteristics and origin of a lava structural type transitional between pahoehoe and aa. *Bull. Volcanol.* **1987**, *49*, 631–641. [\[CrossRef\]](#)
107. Erlund, E.J.; Cashman, K.V.; Wallace, P.J.; Pioli, L.; Rosi, M.; Johnson, E.; Granados, H.D. Compositional evolution of magma from Parícutin Volcano, Mexico: The tephra record. *J. Volcanol. Geotherm. Res.* **2010**, *197*, 167–187. [\[CrossRef\]](#)
108. Pioli, L.; Erlund, E.; Johnson, E.; Cashman, K.; Wallace, P.; Rosi, M.; Delgado Granados, H. Explosive dynamics of violent Strombolian eruptions: The eruption of Parícutin Volcano 1943–1952 (Mexico). *Earth Planet. Sci. Lett.* **2008**, *271*, 359–368. [\[CrossRef\]](#)
109. Patel, J.P.; Brook, M.S. Erionite asbestiform fibres and health risk in Aotearoa/New Zealand: A research note. *N. Z. Geogr.* **2021**, *77*, 123–129. [\[CrossRef\]](#)
110. Gravis, I.; Németh, K.; Twemlow, C.; Németh, B. The Ghosts of Old Volcanoes, a Geoheritage Trail Concept for Eastern Coromandel Peninsula, New Zealand. *Geoconserv. Res.* **2020**, *3*, 40–57. [\[CrossRef\]](#)
111. Güngör, Y. Geoheritage Inventory and Geotourism Studies of Gökçeada (Çanakkale, Western Türkiye). *Geoheritage* **2024**, *16*, 138. [\[CrossRef\]](#)
112. Louz, E.; Rais, J.; Barakat, A.; Barka, A.A.; Nadem, S. Inventory and Assessment of Geosites and Geodiversity Sites of the Ait Attab Syncline (M’goun Unesco Geopark, Morocco) to Stimulate Geoconservation, Geotourism and Sustainable Development. *Quaest. Geogr.* **2023**, *42*, 115–143. [\[CrossRef\]](#)
113. Perotti, L.; Bollati, I.M.; Viani, C.; Zanoletti, E.; Caironi, V.; Pelfini, M.; Giardino, M. Fieldtrips and virtual tours as geotourism resources: Examples from the Sesia Val Grande UNESCO Global Geopark (NW Italy). *Resources* **2020**, *9*, 63. [\[CrossRef\]](#)
114. Szakács, A.; Kovacs, M. Volcanic Landforms and Landscapes of the East Carpathians (Romania) and Their Geoheritage Values. *Land* **2022**, *11*, 1064. [\[CrossRef\]](#)
115. Kereszturi, G.; Grosse, P.; Whitehead, M.; Guilbaud, M.N.; Downs, D.T.; Noguchi, R.; Kervyn, M. Understanding the evolution of scoria cone morphology using multivariate models. *Commun. Earth Environ.* **2025**, *6*, 439. [\[CrossRef\]](#)
116. Vörös, F.; van Wyk de Vries, B.; Guilbaud, M.N.; Görüm, T.; Karátson, D.; Székely, B. DTM-Based Comparative Geomorphometric Analysis of Four Scoria Cone Areas—Suggestions for Additional Approaches. *Remote Sens.* **2022**, *14*, 6152. [\[CrossRef\]](#)
117. Kereszturi, G.; Németh, K. Post-eruptive sediment transport and surface processes on unvegetated volcanic hillslopes—A case study of Black Tank scoria cone, Cima Volcanic Field, California. *Geomorphology* **2016**, *267*, 59–75. [\[CrossRef\]](#)
118. Kervyn, M.; Ernst, G.G.J.; Carracedo, J.C.; Jacobs, P. Geomorphometric variability of “monogenetic” volcanic cones: Evidence from Mauna Kea, Lanzarote and experimental cones. *Geomorphology* **2012**, *136*, 59–75. [\[CrossRef\]](#)
119. Fornaciai, A.; Favalli, M.; Karátson, D.; Tarquini, S.; Boschi, E. Morphometry of scoria cones, and their relation to geodynamic setting: A DEM-based analysis. *J. Volcanol. Geotherm. Res.* **2012**, *217–218*, 56–72. [\[CrossRef\]](#)
120. Inbar, M.; Risso, C. A morphological and morphometric analysis of a high density cinder cone volcanic field-Payun Matru, south-central Andes, Argentina. *Z. Geomorphol.* **2001**, *45*, 321–343. [\[CrossRef\]](#)
121. Hooper, D.M.; Sheridan, M.F. Computer-simulation models of scoria cone degradation. *J. Volcanol. Geotherm. Res.* **1998**, *83*, 241–267. [\[CrossRef\]](#)
122. Wood, C.A. Morphometric analysis of cinder cone degradation. *J. Volcanol. Geotherm. Res.* **1980**, *8*, 137–160. [\[CrossRef\]](#)

Disclaimer/Publisher’s Note: The statements, opinions and data contained in all publications are solely those of the individual author(s) and contributor(s) and not of MDPI and/or the editor(s). MDPI and/or the editor(s) disclaim responsibility for any injury to people or property resulting from any ideas, methods, instructions or products referred to in the content.